INCREASING AIR DEFENSE CAPABILITY BY OPTIMIZING BURST DISTANCE

A THESIS SUBMITTED TO
THE GRADUATE SCHOOL OF NATURAL AND APPLIED SCIENCES
OF
MIDDLE EAST TECHNICAL UNIVERSITY

BY

MEHMET TÜRKUZAN

IN PARTIAL FULLFILLMENT OF THE REQUIREMENTS
FOR
THE DEGREE OF MASTER OF SCIENCE
IN
ELECTRICAL AND ELECTRONICS ENGINEERING

DECEMBER 2010

Approval of the thesis:

INCREASING AIR DEFENSE CAPABILITY BY OPTIMIZING BURST DISTANCE

submitted by **MEHMET TÜRKUZAN** in partial fulfillment of the requirements for the degree of **Master of Science in Electrical and Electronics Engineering Department, Middle East Technical University** by,

Prof. Dr. Canan Özgen _____

Dean, Graduate School of **Natural and Applied Sciences**

Prof. Dr. İsmet Erkmen _____

Head of Department, **Electrical and Electronics Engineering**

Prof. Dr. Erol Kocaoğlan _____

Supervisor, **Electrical and Electronics Engineering Dept., METU**

Examining Committee Members:

Prof. Dr. Mübeccel Demirekler _____

Electrical and Electronics Engineering Dept., METU

Prof. Dr. Erol Kocaoğlan _____

Electrical and Electronics Engineering Dept., METU

Prof. Dr. Kemal Leblebicioğlu _____

Electrical and Electronics Engineering Dept., METU

Assist. Prof. Dr. Afşar Saranlı _____

Electrical and Electronics Engineering Dept., METU

Dr. Hüseyin Yavuz _____

ASELSAN Inc.

Date: _____

I hereby declare that all information in this document has been obtained and presented in accordance with academic rules and ethical conduct. I also declare that, as required by these rules and conduct, I have fully cited and referenced all material and results that are not original to this work.

Name, Last name : MEHMET TÜRKUZAN

Signature :

ABSTRACT

INCREASING AIR DEFENSE CAPABILITY BY OPTIMIZING BURST DISTANCE

Türkuzan, Mehmet

M. Sc., Department of Electrical and Electronics Engineering

Supervisor: Prof. Dr. Erol Kocaoğlan

December 2010, 56 pages

In this thesis, burst distance is optimized to increase air defense capability for systems utilizing airburst munitions. A simulator program is created to use during the study by taking advantage of the MATLAB environment. While creating the simulator program, a munition path model is derived by using fourth order Runge-Kutta method. Then, simulations are conducted at different burst distances and related information are recorded. By using least square optimization method and gathered data, optimum burst distance is found. Moreover, the effects of several factors on optimum burst distances are analyzed, including: the weights of the objectives in the optimization, target dimensions, target range, wind, target position ambiguity, firing angle, and velocity ambiguity after burst. Furthermore, a firing method is proposed. The result of the proposed firing method and the optimum solution are compared and success is presented. To sum up, this study presents a way to find optimum burst distance, analyzes the factors that may affect optimum burst distance, and suggests a firing method for effective shots.

Keywords: Airburst munitions, burst distance optimization, fire control.

ÖZ

HAVA SAVUNMA KABİLİYETİNİN ARTTIRILMASI AMACIYLA PARALANMA MESAFESİ OPTİMİZASYONU

Türkuzan, Mehmet

Yüksek Lisans, Elektrik Elektronik Mühendisliği Bölümü

Tez Yöneticisi: Prof. Dr. Erol Kocaoğlan

Aralık 2010, 56 sayfa

Bu çalışmada, havada paralanan mühimmatla hava savunması yapan sistemlerde etkinliğin arttırılması amacıyla paralanma mesafesi optimizasyonu yapılmıştır. Çalışmada kullanılmak üzere MATLAB ortamından faydalanılarak bir simülatör yazılmıştır. Simulator geliştirme aşamasında mühimmat yolu modeli dördüncü dereceden runge-kutta metodu kullanılarak çıkarılmıştır. Daha sonra farklı mesafelerde paralanma mesafesi simülasyonu yapılarak gerekli veriler toplanmıştır. Bu veriler kullanılarak en küçük kareler metoduyla optimum paralanma mesafesi bulunmuştur. Ayrıca; optimizasyonda kullanılan parametrelerin, hedef boyutunun, hedef uzaklığının, rüzgârın, hedef belirsizliğinin, atış açısının, paralanmadan sonra parçacıkların hızlarındaki değişimin paralanma mesafesine etkileri incelenmiştir. İlaveten, bir de atış şekli önerisinde bulunulmuştur. Bu atış şeklinin vermiş olduğu paralanma mesafesiyle optimum paralanma mesafesi karşılaştırılmıştır. Özetle, bu çalışma optimum paralanma mesafesi bulma yolu göstermiştir. Optimum paralanma mesafesini etkileyen faktörleri incelemiştir. Ayrıca, etkin bir atış yapabilmek için bir atış şekli önerisinde bulunmuştur.

Anahtar Kelimeler: Havada paralanan mühimmatlar, paralanma mesafesi optimizasyonu, atış kontrol.

To My Parents and Love

ACKNOWLEDGEMENTS

I would like to express my sincere thanks and gratitude to my supervisor Prof. Dr. Erol Kocaoğlan for his guidance, valuable advices, and support.

I owe my deepest gratitude to Burak Kekeç and Muharrem Tümçakır for their support and encouragements.

I certainly would like to thank Emin İlker Çetinbaş for his reviews and feedback during the writing process.

I want to express my gratitude to my colleagues at Aselsan Inc.

I want to thank Aselsan Inc. for facilities provided.

I would also like to thank TÜBİTAK for providing me financial support for my study.

Finally, my thanks go to my parents İdris and Türkan, to my wife Ayşe, and to my brother Melih for their endless love, encouragements, and support.

TABLE OF CONTENTS

LIST OF TABLES

TABLES

LIST OF FIGURES

FIGURES

ABBREVIATION LIST

α_t : Attack Angle

$\vec{V}$: Vector Velocity of the Projectile

$\vec{W}$: Vector Velocity of the Wind

S : Projectile Reference Area

ρ : Air Density

C_D : Drag Force Coefficient

$\vec{x}$: Unit Vector Along the Projectile's Rotational Axis of Symmetry

C_{La} : Lift Force Coefficient

d : Projectile Reference Diameter

C_{Npa} : Magnus Force Coefficient

I_y : Projectile Transverse Moment of Inertia

I_x : Projectile Axial Moment of Inertia

$\vec{h}$: Vector Angular Momentum Divided by the Transverse Moment of Inertia

$C_{Nq} + C_{Na}$: Pitch Damping Coefficient

$\vec{g}$: Vector Acceleration Due to Gravity

$\vec{\Lambda}$: Vector Coriolis Acceleration

T : Rocket Thrust Force

m : Mass of the Projectile

r_e : Distance from Projectile Center of Mass to the Rocket Nozzle Exit

CHAPTER 1

INTRODUCTION

1.1 BACKGROUND AND SCOPE OF THE THESIS

“Missile hurling was a skilled craft thousands of years before writing was developed…” [1] Throughout the history, human beings needed to fight for food or defense. At Stone ages, they used hurled stones and then they created spears and javelins. After the invention of gunpowder, firearms were invented, thus weapons have been changed. Lethality of weapons and effective ranges of the weapons have been improved with time. However, as the effective ranges of these weapons increased, it became more difficult to accurately aim these weapons. This problem is named as “Fire Control Problem” and defined as the firing of a projectile from a weapon in order to hit a selected target [1].

Parallel to the development of guns; munitions are improved and diversified. In this study, model is derived for medium caliber ammunition. 20 millimeters (mm) through 60mm ammunition is grouped as medium caliber ammunition which was first used in the World War I. Previously the main purpose of this size ammunition involved an anti aircraft role. Its early use in ground applications was against lightly armored vehicles [3].

Conventional medium caliber ammunition is grouped into two; high explosive ammunitions, which are used in point detonating or point detonating delay mode, and airburst ammunitions. In World War II, airburst munitions of the time were used as anti aircraft. Manually aimed guns, which fire fragmental (airburst) munitions, had provided an effective air defense against bomber aircrafts of that

time. The most known ones were the Germans flak (fliegerabwehrkanone) guns which fired grooved projectiles [9, 18].

Medium caliber ammunition has improved over time. Increment of the ground anti armor penetration requirements during the 1990's gave rise to the high performance armor piercing ammunition. The technological advances had improved airburst munitions [3]. Once more they would be used against aircrafts like in the World War II. Today, the most effective air defense systems are accepted as the ones deploying air bursting munitions, with their greater area of engagement [9].

In the literature, there are some studies about airburst munitions, such as; the burst time optimization [8, 13, 19], various ways of setting the fuse timer [6, 7, 8]. About the burst time optimization, general tendency is on keeping the optimum burst distance constant. There are two ways of setting fuse timer which are; setting timer at the muzzle of the gun [6, 8] and setting timer as late as possible at somewhere on its flight path [7]. Both of these methods require the optimum burst distance. In this thesis, optimum burst distance is found. Moreover, the parameters that may affect optimum burst distance is analyzed which are: firing angle, range of the target, dimensions of the target, presence of wind, importance of the objectives, ambiguity in the target position, and variation of the particles velocity after burst. Additionally, a firing method is proposed. However; target position estimation, firing angle calculation, target and munition path calculations are not in the scope of this thesis. They are implemented to provide inputs for the study.

1.2 OUTLINE OF THE THESIS

In this thesis, optimum burst distance of airburst munitions is studied. Simulations are carried out and data is gathered for optimization. In the simulations, target movement is not tracked and it is not considered because the studies like tracking the target and estimating the target position are well known studies which had been

already studied a lot. Thus, during the simulations, intersection point of the munition path and target path is assumed as given.

In Chapter 2, fire control problem and optimization problem is explained. Airburst munitions are described and other types of munitions are mentioned briefly as background information. Least square optimization method and fourth order Runge Kutta method is presented. Literature survey in the field of airburst munitions is presented by mentioning several outstanding studies briefly.

Chapter 3 derives the system model, describes the cost function, shows the proposed firing method, and presents the simulator program written in MATLAB. Therefore, assumptions about system model derivation are given in this part.

In Chapter 4, optimization problem is solved. Results are presented. The effects of the parameters on optimum burst distance are analyzed. Proposed firing method's solution is compared to the optimum solution.

Chapter 5 concludes the study by giving a summary of the work done. It also mentions possible future work to guide the researchers in this area.

CHAPTER 2

LITERATURE SURVEY

This chapter gives general information about the field of the study and background on the subject. In Section 2.1, general information about fire control is presented. In Section 2.2, airburst munitions are described. In Section 2.3, general information about optimization problem is presented. In Section 2.4, Runge-Kutta method is presented. In the last section, general patented methods about increasing effectiveness of the systems that use airburst munitions are presented.

2.1 FIRE CONTROL

Launching a projectile from a gun system to hit a target is called the fire control problem. Fire control mainly means offsetting the gun direction from line of sight in order to solve the fire control problem which is hitting the selected target as illustrated in Figure 2-1 [1]. In fire control problem, both target and gun system may be moving.

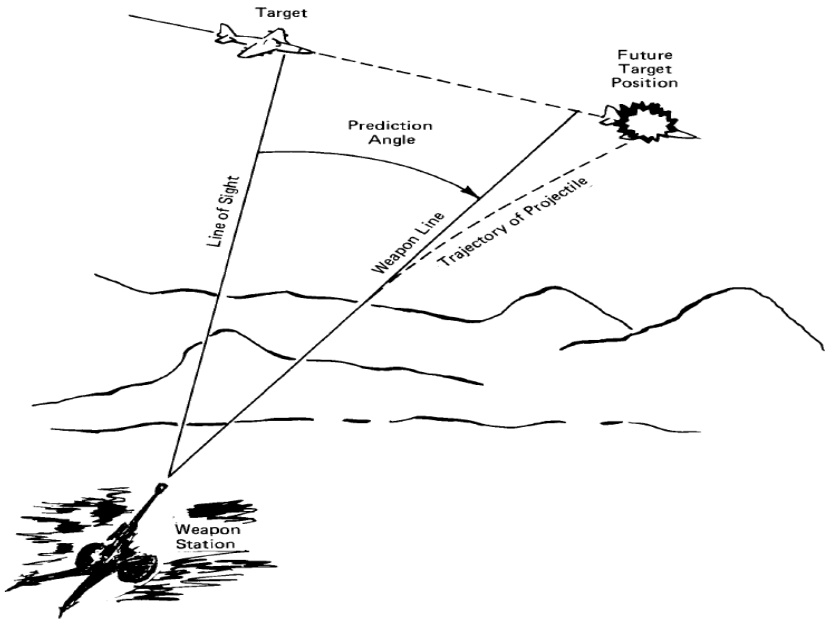

Figure 2-1: Illustration of general fire control problem [1]

Offset angle is called prediction angle that is the angle between line of sight and gun direction, called weapon line. Prediction angle is the solution provided by a fire control system by available information. This solution, prediction angle, is achieved as the result of offset components in elevation and azimuth. Solution data are applied up to the time of firing for guns and rocket launchers, whereas for guided missiles, solution data are also applied at some intervals or continuously after firing [1].

Fire control has mainly three functions. These functions are; acquiring appropriate input data, calculating the elevation and azimuth angles required for the projectile to intersect the target, and applying these angles to the fire control mechanism to position the gun correctly. These three functions are associated with acquisition and tracking systems, computing systems and gun pointing systems.

In some situations fire control includes solution of two additional problems. The first problem is maintaining awareness of the gun-target situation which means that gun turret is following the target. Gun is always ready to fire. This problem is more

significant for fast targets. In this case, gun aims to the target all the time, since aiming just before firing is sometimes physically impossible due to the need of very fast movements of gun turret. The second problem is controlling the time and volume of fire to achieve maximum effectiveness of fire and minimize waste of ammunition, which involves making projectiles explode when they reach the vicinity of the target by means of time fuzes preset by a fuze-time computer.

Thus, fire control may be broadly defined as quantitative control over one or more of the following items to deliver effective weapon fire on a selected target:

1. The direction of launch

2. The time and volume of fire

3. The detonation of the missile [1]

The first item, namely direction of launch, and the second item namely time and volume of fire are subjects of other studies. The detonation of missile control is the problem of the systems which utilize airburst munitions. In this thesis, airburst munitions are considered and detonation of missile control is the subject of this study.

2.2 AIRBURST MUNITIONS

Munitions are diversified according to their sizes; small caliber, medium caliber and large caliber. Small caliber munitions diameter are smaller than 20mm. Medium caliber munitions are considered as 20mm through 60mm and large caliber munitions are bigger than 60mm. Munitions are also classified by the types of their fuzes, namely; impact, time, command, inferential and proximity. Impact fuzes operate as munitions hit the target, time fuzes operate after a predefined time passes, command fuzes operate by a signal from a remote controller, inferential fuzes function if preconditions are met, and proximity fuzes function if munitions are at defined distance [20].

Airburst munitions have two types of fuzes, mentioned above, which are time fuzes and command fuzes [7, 8]. Since this thesis concentrates on the optimum burst distance, the fuze type of the munition is not important, as long as time of burst is controlled.

The concept of airburst munitions is to burst munitions in the air above the target or in front of the target. The aim is to put maximum fragments on the target area. Since airburst munitions have lots of fragments, their probability of hit is greater than a single piece munition. Although, the main aim of airburst munitions is increasing the probability of hit, they may be used to engage more targets which are close to each other, if it is necessary [2].

In Figure 2-2, 35mm base fused time-programmable airburst munition is shown. As seen from the figure, there are a lot of sub projectiles inside.

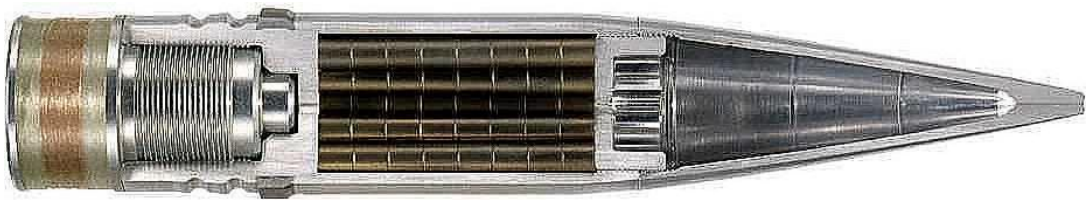

Figure 2-2: 35mm time programmable airburst munition [10]

In Figure 2-3, the parts of the munition are shown. Different munitions include different number of sub projectiles inside. The one in the figures includes 152 tungsten sub projectiles.

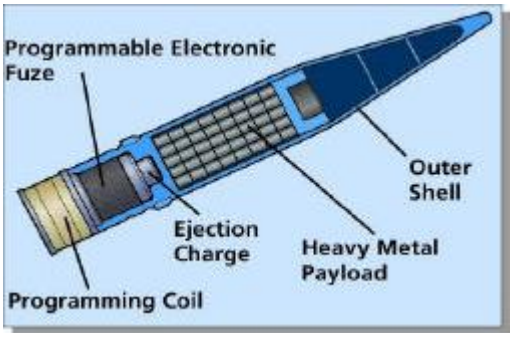

Figure 2-3: Description of the parts [10]

In Figure 2-4, the configuration of a system utilizing airburst munitions is shown. The working principle of the system can be summarized as follows: After detection of target, position and velocity information are sent to gun computer. Then, gun makes required calculations including target path estimation, time of flight and burst time. Finally, munition is fired.

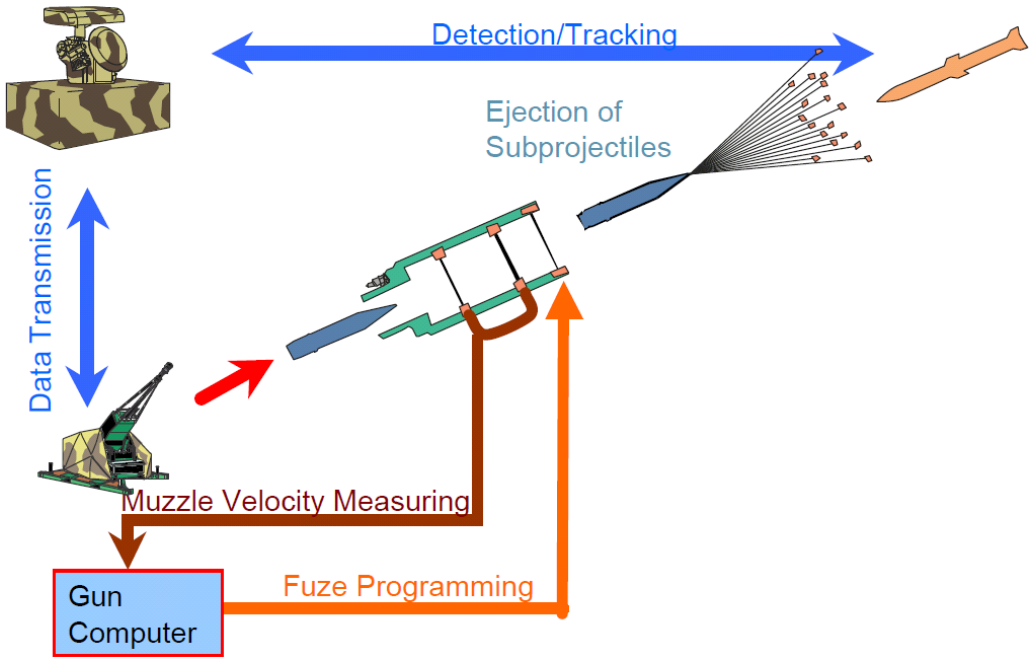

Figure 2-4: General airburst system configuration [10]

In Figure 2-5, the end part of the cannon of the above configuration is shown. This device is used for calculating the actual muzzle velocity of the projectile in several systems. The device has three coils and the working principle of the device is the following. When munition is sensed by first coil, gun computer starts a timer. When munition is sensed by second coil, gun computer stops the timer. With this information, the computer calculates actual muzzle velocity. Then gun computer calculates burst time and set this time on the fuze using the third coil.

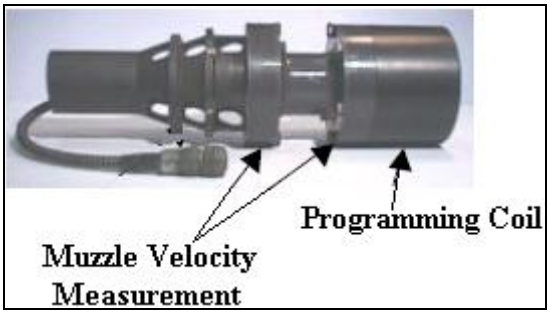

Figure 2-5: End part of cannon [10]

There is a different system that also fires airburst munitions. Their munitions are of different kinds. One of them is trigged by a specific radio signal, in which the system detects tracks of trajectories and gives the fire command accordingly. After firing, both the target and the munition are tracked with radars. At the best point fire signal is sent to burst the munition.

2.3 OPTIMIZATION PROBLEM

Optimization problem is defined with the following quadruple (*S, m, v, C*). Where

- *S* is a set of solutions (burst distances),
- $m(x)$ is the set of objective parameters, given an instance $x \in S$,
- $v(x)$ is the set of cost values, given an instance $x \in S$,

- C is the cost function.

The aim is to find an optimal solution, $X_o \in S$, in the set of solutions *S:*

$$v(x) = C(x) \mid x \in S$$
$$v(X_o) = \min v(x) \mid x \in S \quad (2\text{-}1)$$

In this thesis, optimization is used to find burst distance. Simulations are carried on, objective parameters are recorded. Then, these records are processed by the cost function to find the optimum solution. The cost function of the optimization is created by using least squares optimization method.

2.3.1 LEAST SQUARES OPTIMIZATION METHOD

The cost function of least square optimization problems is expressed as a sum of squares [29]. The best fitting curve, according to least squares, has the minimal sum of the deviations squared (least square error) from a given set of data [31].

There are a set of data points (x_1, y_1), (x_2, y_2), ..., (x_n, y_n) where x is the independent variable and y is the dependent variable. The deviations (error) d of the fitting curve $f(x)$ from each data point are $d_1 = y_1 - f(x_1)$, $d_2 = y_2 - f(x_2)$, ..., $d_n = y_n - f(x_n)$. According to the method of least squares, the best fitting curve is the curve which satisfies the minimum squared error as in Equation(2-2) [31].

$$\Pi = d_1^2 + d_2^2 + ... + d_n^2 = \sum_{i=1}^{n} d_i^2 = \sum_{i=1}^{n} [y_i - f(x_i)]^2 \quad (2\text{-}2)$$

In this thesis, least squares method is used to derive cost function of the optimization. Actual values of the objective parameters are subtracted from the ideal objective parameters. Each deviation is squared and they are summed up as formulated in Equation (3-15). Minimum value means minimum deviation from the ideal in the least squares sense.

2.4 RUNGE-KUTTA METHOD

In numerical analysis, Runge-Kutta methods are an important family of implicit and explicit iterative methods. Runge-Kutta methods are used for the approximation of the solutions of ordinary differential equations [31]. An ordinary differential equation of the form of Equation (2-3) can be iteratively solved with the 4th order Runge-Kutta method whose formula is given by Equation (2-4).

$$\frac{dy}{dx} = f(x, y)$$

$$y(0) = y_0 \tag{2-3}$$

$$\begin{aligned} y_{i+1} &= y_i + \frac{1}{6}(k_1 + 2k_2 + 2k_3 + k_4)h \\ h &= x_{i+1} - x_i \\ k_1 &= f(x_i, y_i) \\ k_2 &= f(x_i + \frac{1}{2}h, y_i + \frac{1}{2}k_1 h) \\ k_3 &= f(x_i + \frac{1}{2}h, y_i + \frac{1}{2}k_2 h) \\ k_4 &= f(x_i + h, y_i + k_3 h) \end{aligned} \tag{2-4}$$

Hence, y_{i+1} is calculated by the present value y_i plus the product of the interval h and an estimated slope. This estimated slope is a weighted average of slopes:

- k_1 is the slope at the beginning of the interval,
- k_2 is the slope at the midpoint of the interval, using slope k_1 to determine the value of y at the point $t_n + h/2$ using Euler's method,
- k_3 is again the slope at the midpoint, but now using the slope k_2 to determine the y-value,
- k_4 is the slope at the end of the interval, with its y-value determined by using k_3 in previous step [31].

In this thesis, fourth order Runge Kutta method is used to solve the iterative differential equations of the flight path model.

2.5 LITERATURE SURVEY ABOUT AIRBURST MUNITIONS

In literature, there are some patents awarded for increasing effectiveness of airburst munitions. All these patented methods concentrate on the calculation of burst time. In this section, the differences and similarities of these methods are presented.

One patented method [8] aims at determining burst time of airburst munitions. It is possible that hit probability of airburst munitions can be improved by using this method. In order to score better hit probabilities, method suggests keeping optimum distance between the burst point and the hit point constant. The method calculates a time correction value for keeping burst distance constant. Calculation of time correction value is basically found by multiplying the velocity difference between estimated muzzle velocity and actual muzzle velocity by a constant, as shown in Equation(2-5)[8, 12, 13, 19]. $V_{estimated}$ is the average muzzle velocity of the previous shots. $t_{calculated}$ is the burst time calculated with a $V_{estimated}$ muzzle velocity. t_{burst} is the burst time corrected by measuring actual muzzle velocity.

$$t_{burst} = t_{calculated} + \kappa(V_{estimated} - V_{actual}) \tag{2-5}$$

The actual muzzle velocity is measured by a device located at the muzzle of the gun as shown in Figure 2-5. Burst time is corrected and the success of the projectile is improved [8, 12, 13, 19].

There is a patented method [6] that measures muzzle velocity by counting revolutions of the projectile in the barrel. Counting the revolutions of the projectile in the barrel is the difference of the present method from the above mentioned method. This method also keeps the optimum burst distance constant. The method uses a device which measures the revolution of the projectile. By this revolution counting device actual muzzle velocity is measured. The method says that defined number of revolution is normally completed in time *t*. The revolutions counting

device counts defined revolutions in time t_m. Then, Equation (2-6) gives the corrected burst time calculation as:

$$T_{burst} = T_{estimated} + \kappa(t_m - t) \quad (2\text{-}6)$$

κ is the constant. T_{burst} is the corrected time. $T_{estimated}$ is the estimated burst time depending on the previous experiments [6].

A third patented method [12] differs from the others by its device for transferring information to projectiles. This device is placed in the barrel of the gun. Burst time depends on the position of this device in the barrel. Thus, performance of the shot can be tuned by changing the position of the device. Furthermore, this invention uses many computing units and filter blocks to calculate burst time better in order to maintain optimal burst distance.

Another patented invention [7] differs from the others by watching projectile and target actively. This method determines burst time by keeping optimum burst distance constant like others. However, projectile is remotely fragmentable. Burst time is not downloaded to the projectile. Radar and gun computer actively watch the projectile and target. When distance between them is equal to the optimum burst distance, an RF signal is sent and projectile is bursted.

The above mentioned methods all assume that an optimum burst distance is available. They suggest different methods to keep optimum burst distance as it is. However, there is no publicly available study about finding optimum burst distance. Hence, this thesis concentrates on optimum burst distance. Therefore, the result of this study can be used by all methods mentioned.

CHAPTER 3

DERIVING THE SYSTEM MODEL

In this chapter, derivations of the models which are used during the study are presented. Firstly, munition path model is derived. Initial model includes all forces that act on the projectile. However, the model used in the simulations is a simplified version of the initial model. The simplification is done by using assumptions given in Section 3.1.

Next, the cost function to be optimized is presented. Least-square error minimization method is used to find the optimum burst distance.

After cost function presentation, two different firing methods are presented. First firing method is for the case when target location is known with zero error. Second firing method is for the case when target location is not known perfectly.

Finally, the program written in MATLAB to solve equations that are derived in this chapter is presented.

3.1 ASSUMPTIONS

Simplification is very important for modeling [28]. Target is assumed as an ellipsoid in this thesis. As mathematical definition of an ellipsoid is simple and easy to express, target is assumed to be of ellipsoid shape.

Air density and gravitational acceleration are assumed as constant. In Figure 3-1, there is an illustration of a projectile with trajectory path. The angle between the axial direction of a projectile and the tangent to the trajectory is the attack angle. Attack angle is assumed as zero during the simulations. Besides, projectile is

assumed as non-rotational. Since, the study concentrates on very short range air defense, those last two assumptions have minor effects on the projectile path [26].

There are some assumptions to define projectile and its behavior. Projectile includes 181 particles. After burst, particles fly in a cone shape with 10 degrees apical angle [8]. Furthermore, particles gain 150 m/s velocity in average due to the burst effect. To define coordinate start point, muzzle of the gun is assumed as the origin of the coordinate system.

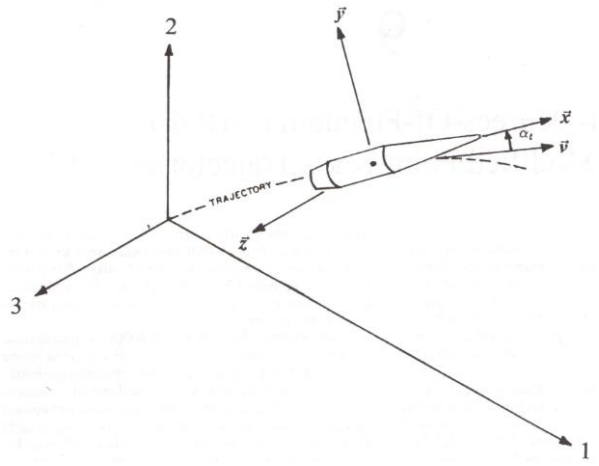

Figure 3-1: Coordinate system for six-degrees-of-freedom trajectories [26]

3.2 FLIGHT PATH MODEL

The aim of this part is to derive the flight path model of an airburst munition. Firstly, a model that includes all forces, which is known as six degrees of freedom trajectory model, is presented as given in Equation (3-1). Then, the equation is simplified by introducing some assumptions.

The six-degrees-of-freedom vector differential equations of motion, for a rigid, rotationally symmetric projectile acted on by all significant aerodynamic forces are summarized in Equation(3-1) [26].

$$\frac{d\vec{V}}{dt} = -\frac{\rho v S C_D}{2m}\vec{v} + \frac{\rho S C_{La}}{2m}[v^2\vec{x} - (\vec{v}\bullet\vec{x})\vec{v}] - \frac{\rho S d C_{Npa}}{2m}\left(\frac{I_y}{I_x}\right)\left(\vec{h}\bullet\vec{x}\right)\left(\vec{x}\times\vec{v}\right)$$
$$+\frac{\rho v S d(C_{Nq}+C_{Na})}{2m}\left(\vec{h}\times\vec{x}\right) + \vec{g} + \vec{\Lambda} + \frac{gT}{m}\vec{x} + \left(\frac{I_y}{mr_t} - \frac{\dot{m}r_e}{m}\right)\left(\vec{h}\times\vec{x}\right) \quad (3\text{-}1)$$

In this equation, $\vec{V}$ is the velocity vector of the projectile with respect to the Earth fixed coordinate system. $\vec{W}$ is the velocity vector of the wind with respect to the Earth fixed coordinate system. $\vec{v}$ is the velocity vector of the projectile with respect to the air $(\vec{v} = \vec{V} - \vec{W})$. The first term $(-\frac{\rho v S C_D}{2m}\vec{v})$ in Equation (3-1) is related to drag force, and v indicates the norm of the vector $\vec{v}$. S is the projectile reference area, ρ is the air density, m is the mass and C_D is the drag force coefficient [26].

The second term $(\frac{\rho S C_{La}}{2m}[v^2\vec{x} - (\vec{v}\bullet\vec{x})\vec{v}])$ is related to the lift force. $\vec{x}$ is the unit vector along the projectile's rotational axis of symmetry. C_{La} is the lift force coefficient. $\bullet$ is the dot product operator [26].

The third term $(-\frac{\rho S d C_{Npa}}{2m}\left(\frac{I_y}{I_x}\right)\left(\vec{h}\bullet\vec{x}\right)\left(\vec{x}\times\vec{v}\right))$ in Equation (3-1) is related to the magnus force. d is the projectile reference diameter. C_{Npa} is the magnus force coefficient. I_y is the projectile transverse moment of inertia. I_x is the projectile axial moment of inertia. $\vec{h}$ is the vector angular momentum divided by the transverse moment of inertia and $\times$ is the cross product operator [26].

The fourth term $(\frac{\rho v S d(C_{Nq}+C_{Na})}{2m}\left(\vec{h}\times\vec{x}\right))$ in Equation (3-1) is related to the pitch damping force. $C_{Nq}+C_{Na}$ is the pitch damping coefficient [26].

$\vec{g}$ is the acceleration vector due to gravity. $\vec{\Lambda}$ is the coriolis acceleration vector. $\frac{gT}{m}\vec{x}+\left(\frac{I_y}{mr_t}-\frac{\dot{m}r_e}{m}\right)\left(\vec{h}\times\vec{x}\right)$ are the rocket related forces. T is the rocket thrust force. m is the projectile mass. r_e is the distance from the center of mass of the projectile to the rocket nozzle exit [26].

Equation (3-1) is a general expression. We will explain five simplifications of Equation (3-1) for our own problem. The simplifications are done by the following three assumptions:

1. h is zero,

2. angle of attack which is presented in Figure 3-1 by α_t is zero,

3. $\vec{\Lambda}$ is zero.

This study concentrates on airburst munitions. Airburst munition mass is constant during the flight. They are not rocket like munitions. So, $\frac{gT}{m}\vec{x}$ is zero, as T is zero. $\left(\frac{I_y}{mr_t}-\frac{\dot{m}r_e}{m}\right)\left(\vec{h}\times\vec{x}\right)$ is zero, since used projectile is non-rotational which means $\vec{h}$ is zero.

The second term ($\frac{\rho SC_{La}}{2m}[v^2\vec{x}-(\vec{v}\bullet\vec{x})\vec{v}]$) in the Equation(3-1) diminishes to zero. The reason can be simply explained as: The angle of attack is taken as zero in this study, so $\vec{x}$ and $\vec{v}$ will have the same direction. As a result $\vec{v}\bullet\vec{x}=|v|$, norm of $\vec{v}$. Hence, $v^2\vec{x}-(\vec{v}\bullet\vec{x})\vec{v}$ can be written as $v^2\vec{x}-|v|\vec{v}$ which is equal to $v^2\vec{x}-v^2\vec{x}$, and hence the desired result. Another consequence of zero angle of attack is that

$\vec{x} \times \vec{v} = 0$, since $\vec{x}$ and $\vec{v}$ have the same orientation. Thus, the third term $(-\frac{\rho S d C_{Npa}}{2m}\left(\frac{I_y}{I_x}\right)\left(\vec{h} \bullet \vec{x}\right)\left(\vec{x} \times \vec{v}\right))$ in the Equation (3-1) diminishes to zero.

Since the projectile used in the study is non-rotational, $\vec{h}$ is zero, hence the fourth term $(\frac{\rho v S d (C_{Nq} + C_{Na})}{2m}\left(\vec{h} \times \vec{x}\right))$ in the Equation(3-1) becomes zero.

The force due to coriolis is ignorable compared to gravitational and air drag forces. Therefore, coriolis force is taken as zero during the study. Finally, six degrees-of-freedom equations converge to the equations of Point-Mass trajectory given in Equation (3-2).

$$\frac{d\vec{V}}{dt} = -\frac{\rho v S C_D}{2m}\vec{v} + \vec{g} \tag{3-2}$$

Trajectory formulation is derived. Then, the trajectory model of the munition which is used during the study should be defined. Firstly, the state vector of the model is presented in Equation (3-3).

$$\Im = \begin{bmatrix} x \\ \dot{x} \\ y \\ \dot{y} \\ z \\ \dot{z} \end{bmatrix} \tag{3-3}$$

The state space is six dimensional Cartesian space, $S = \Re^6$. The state vector $\Im \in S$ consists the position $\Im_p \in \Re^3$, and the velocity $\Im_v \in \Re^3$ [28]. The general formulation of the states are presented in Equation (3-4) and Equation (3-5).

$$\begin{aligned} \dot{\Im}_p &= \Im_v \\ \dot{\Im}_v &= g - \rho\gamma \,|\, \Im_v \,|\, \Im_v \end{aligned} \tag{3-4}$$

(3-5)

Above mentioned iterative flight path differential equations are solved by fourth order Runge-Kutta integration method.

X, Y and Z components of the muzzle velocity is given by Equation (3-6) where V_0 is the muzzle velocity and θ is the firing angle in the Y-Z plane.

$$V_Z = V_0 \cos\theta$$

$$V_Y = V_0 \sin\theta \tag{3-6}$$

$$V_X = 0$$

The initial condition vector is then given as:

$$\Im(0) = \begin{bmatrix} 0 \\ V_X \\ 0 \\ V_Y \\ 0 \\ V_Z \end{bmatrix} \tag{3-7}$$

Whereas Equation (3-8) given below indicates the accelerations:

$$\begin{aligned} \frac{dV_Z}{dt} &= -\rho\gamma V_Z^2 \\ \frac{dV_Y}{dt} &= g - \rho\gamma V_Y^2 \\ \frac{dV_X}{dt} &= -\rho\gamma V_X^2 \end{aligned} \tag{3-8}$$

The value of state vector at the end of one time step Δt will then be given as:

$$\Im(\Delta t) = \Im(0) + \frac{1}{6}(k_1 + 2k_2 + 2k_3 + k_4)\Delta t$$

In the above equation, the k_i values (i=1, 2, 3, 4) are found by using Equation (3-9).

$$
\begin{aligned}
k_1 &= f(\Im(0),0) \\
k_2 &= f(\Im(0)+k_1\frac{\Delta t}{2},\frac{\Delta t}{2}) \\
k_3 &= f(\Im(0)+k_2\frac{\Delta t}{2},\frac{\Delta t}{2}) \\
k_4 &= f(\Im(0)+k_3\Delta t,\Delta t)
\end{aligned}
\tag{3-9}
$$

Using functions $f(\,)$ and $\Im(\,)$, the explicit form of k_i values are obtained as:

$$
k_1 = f(\Im(0),0) = \begin{bmatrix} V_X \\ -\rho\gamma V_X^2 \\ V_Y \\ g-\rho\gamma V_Y^2 \\ V_Z \\ -\rho\gamma V_Z^2 \end{bmatrix}
\tag{3-10}
$$

$$k_2 = f(\Im(0) + k_1\frac{\Delta t}{2}, \frac{\Delta t}{2}) = \begin{bmatrix} V_X \\ -\rho\gamma V_X^2 \\ V_Y \\ g - \rho\gamma V_Y^2 \\ V_Z \\ -\rho\gamma V_Z^2 \end{bmatrix} + k_1\frac{\Delta t}{2} = \begin{bmatrix} V_X(1+\frac{\Delta t}{2}) \\ -\rho\gamma V_X^2(1+\frac{\Delta t}{2}) \\ V_Y(1+\frac{\Delta t}{2}) \\ (g - \rho\gamma V_Y^2)(1+\frac{\Delta t}{2}) \\ V_Z(1+\frac{\Delta t}{2}) \\ -\rho\gamma V_Z^2(1+\frac{\Delta t}{2}) \end{bmatrix} \tag{3-11}$$

$$k_3 = f(\Im(0) + k_2\frac{\Delta t}{2}, \frac{\Delta t}{2}) = \begin{bmatrix} V_X \\ -\rho\gamma V_X^2 \\ V_Y \\ g - \rho\gamma V_Y^2 \\ V_Z \\ -\rho\gamma V_Z^2 \end{bmatrix} + k_2\frac{\Delta t}{2} = \begin{bmatrix} V_X(1+\frac{\Delta t}{2}(1+\frac{\Delta t}{2})) \\ -\rho\gamma V_X^2(1+\frac{\Delta t}{2}(1+\frac{\Delta t}{2})) \\ V_Y(1+\frac{\Delta t}{2}(1+\frac{\Delta t}{2})) \\ (g - \rho\gamma V_Y^2)(1+\frac{\Delta t}{2}(1+\frac{\Delta t}{2})) \\ V_Z(1+\frac{\Delta t}{2}(1+\frac{\Delta t}{2})) \\ -\rho\gamma V_Z^2(1+\frac{\Delta t}{2}(1+\frac{\Delta t}{2})) \end{bmatrix} \tag{3-12}$$

$$k_4 = f(\Im(0) + k_3\Delta t, \Delta t) = \begin{bmatrix} V_X \\ -\rho\gamma V_X^2 \\ V_Y \\ g - \rho\gamma V_Y^2 \\ V_Z \\ -\rho\gamma V_Z^2 \end{bmatrix} + k_3\Delta t = \begin{bmatrix} V_X(1+\Delta t(1+\frac{\Delta t}{2}(1+\frac{\Delta t}{2}))) \\ -\rho\gamma V_X^2(1+\Delta t(1+\frac{\Delta t}{2}(1+\frac{\Delta t}{2}))) \\ V_Y(1+\Delta t(1+\frac{\Delta t}{2}(1+\frac{\Delta t}{2}))) \\ (g - \rho\gamma V_Y^2)(1+\Delta t(1+\frac{\Delta t}{2}(1+\frac{\Delta t}{2}))) \\ V_Z(1+\Delta t(1+\frac{\Delta t}{2}(1+\frac{\Delta t}{2}))) \\ -\rho\gamma V_Z^2(1+\Delta t(1+\frac{\Delta t}{2}(1+\frac{\Delta t}{2}))) \end{bmatrix} \tag{3-13}$$

These calculations are performed for each time step to iterate states forward until the burst of the munition. Then, at burst instant the effect of the burst is added to the states and calculations start again until the particles hit to the target.

Figure 3-2 illustrates the ejection of subprojectiles at burst instant. The ejection of subprojectiles can be assumed to start with firing the munition from the gun. Munition flies until it reaches to the burst point. After burst, 181 particles start to fly in a cone shape with 10 degrees apical angle. Each particle has a flight path and these paths are traced by the formulation which is previously given. Firstly, initial states of the particles are defined. Positions of the particles are all the same, namely the burst point. However, velocities of the particles are different, and are given as shown by Equation (3-14). From this point, each particle is traced as mentioned in the equations from 3-8 to 3-13.

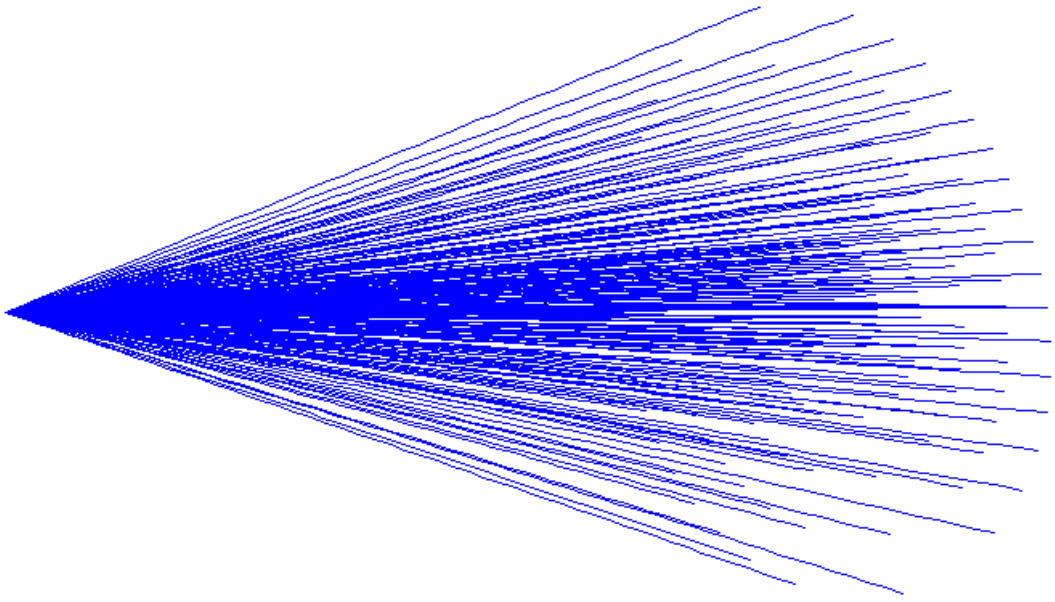

Figure 3-2: Ejection of subprojectiles, plotted by simulator program in MATLAB

Figure 3-3 is the illustrative picture of the particles position a little after the burst. It is created by using MATLAB.

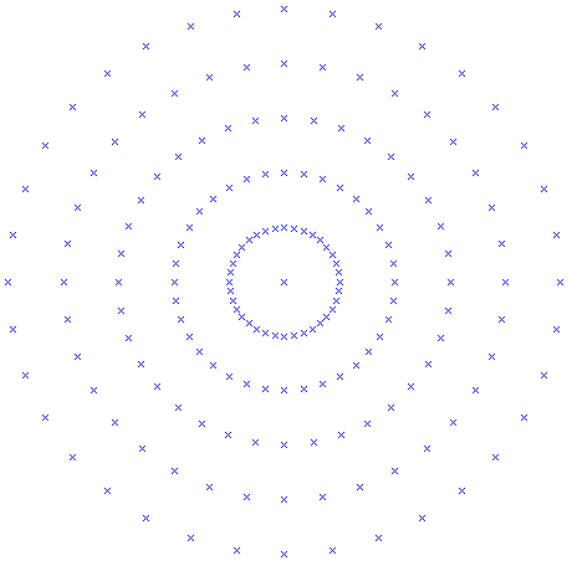

Figure 3-3: An illustration of subprojectile dispersion

After burst, particles are scattered in an order. There are 36 particles on each circle. Their models are given in Equation (3-14).

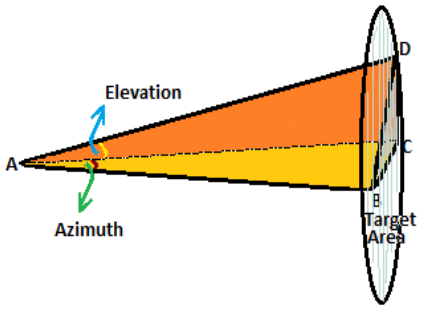

Figure 3-4: 3D subprojectile component illustration

In Figure 3-4, $|AD|$ is the path of the subprojectiles. In this figure, it is shown that path has three components, namely X, Y and Z. The distance $|AB|$ is the distance from burst point, A, to the center of the covered area, B. The direction from point A

to B is the direction of the Z component of the sub-projectiles. The direction from point B to point C is the direction of the X component of the sub-projectiles. And the direction from C to D is the Y component direction. In Equation (3-14), ϕ is the elevation angle, φ is the azimuth angle, θ_B is the elevation angle from -5 to 5 degrees and is used for creating the cone shape. 150 m/s is the velocity increment gained by particles due to burst.

$$V_{Total} = \sqrt{V_X^2(t_{burst}) + V_Y^2(t_{burst}) + V_Z^2(t_{burst})}$$
$$V_{Xp}(t) = (V_{Total} + 150)\cos(\theta_B + \phi)\sin(\varphi)$$
$$V_{Yp}(t) = (V_{Total} + 150)\sin(\theta_B + \phi) - gt \qquad (3\text{-}14)$$
$$V_{Zp}(t) = (V_{Total} + 150)\cos(\theta_B + \phi)\cos(\varphi)$$

In Equation (3-14), t is taken as zero at the time of burst. The state vector is refreshed at the burst, and calculations performed for munition are repeated for particles to find their path after burst.

3.3 COST FUNCTION

During the study, least square method is used for optimization. The variables of the optimization process are hit velocity, number of particles that hit the target and coverage. The weights of the objectives changes with respect to the target. Because, some targets are stronger, penetration of the sub-projectile will be satisfactory if velocity is higher, and for some weak targets, penetration is satisfactory for low speeds so the important components are distribution and coverage. Increasing number of sub-projectiles which hit the target is a common need for all types of targets. Equation (3-15) is a general least squares cost function formulation. The aim is to find the burst distance which minimizes the cost function value. The weights of the objective parameters are a, b, and c in Equation (3-15). Maximum velocity is determined separately for each simulation, the only exception being the simulation where the change of burst distance with respect to firing angle is investigated. In the above mentioned exceptional case, the maximum velocity is

chosen as the same for each calculation. Maximum coverage is %100, and maximum number of particles is 181.

$$C = a(\max\_hitVelocity - actual\_hitVelocity)^2 + b(100 - Coverage)^2 + c(totalParticles - particlesWhichHit)^2 \quad (3\text{-}15)$$

During the study, the weights are selected as equal with, a=b=c=1. This choice indicates that the effects of the different deviations have equal importance. To investigate the effects of cost function weights on burst distance change, a separate study is conducted in Chapter 4.

3.4 A FIRING METHOD IN THE CASE OF PERFECT TARGET LOCALIZATION

In this part, a firing method is presented. The success of the method is shown in Chapter 4.

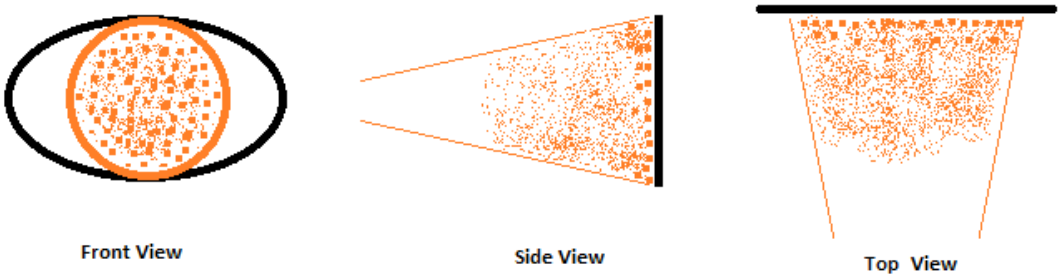

Figure 3-5: The aim of the firing method is illustrated

Figure 3-5, illustrates the aim of the firing method. Since target position is perfectly known, hit probability is 100%. Thus, kill probability should be increased. To increase the kill probability, number of particles that hit the target should be maximized. Moreover, coverage should be maximized to give damage more parts of the target, since the chance of survival for targets decreases with increasing

affected area. On the other hand, if hit velocity is not enough to give the desired damage, burst distance is decreased. So, coverage is decreased.

At Section 3.2, the models of the sub-projectiles were derived. Target surface equation is given to be as:

$$\frac{(X - X_{target})^2}{R_x^2} + \frac{(Y - Y_{target})^2}{R_y^2} + \frac{(Z - Z_{target})^2}{R_z^2} = 1 \quad (3\text{-}16)$$

The trajectory of the munition is found iteratively and positions of the particles are known at each iteration. In Equation (3-16): X, Y, and Z are replaced with the positions of particles. When the result is equal to or smaller than 1, particle hits the target. In other words, particles are checked for hits at each iteration. The cost function is calculated for each assumed burst distance, and as a result, the burst distance giving the minimum cost is obtained.

3.5 A FIRING METHOD IN THE PRESENCE OF TARGET LOCALIZATION ERRORS

In this part, the "firing method", mentioned in Section 3.4, is changed by handling localization errors. That means that the position of the target is not known exactly. The center of the target is assumed to have an uncertainty of Gaussian type. This uncertainty is shown in Figure 3-6.

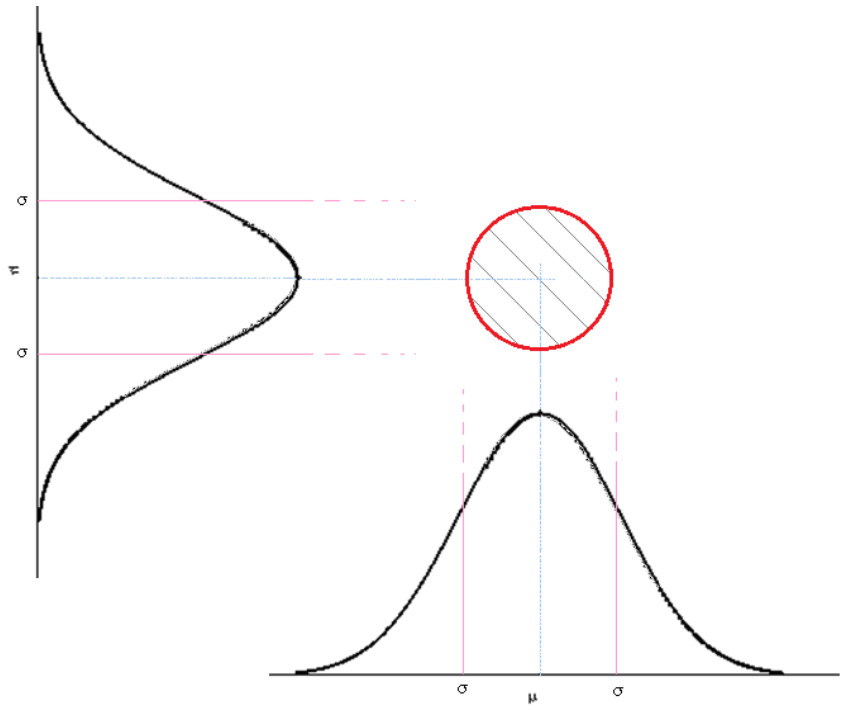

Figure 3-6: The area where target centre position exists mostly

In Figure 3-6, covered area represents the area where target center position exists mostly. The covered area is illustrated as a circle, however it is an ellipse. The aim of this firing method can be shown by a circle whose radius is presented in Figure 3-7 with a red line.

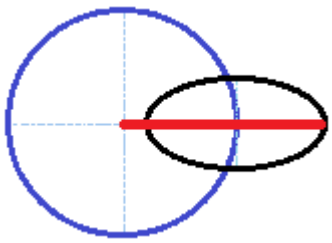

Figure 3-7: The radius of the aimed circle

In Figure 3-7, circular area indicates the area where target center position mostly exists, it is the circle shown in Figure 3-6. The ellipse represents the target. The red line shows the radius of the worst case circle that is the aim of the firing method. The start point of the line is the center of the circular area and the end point of the red line is on the ellipse as shown in the Figure 3-7.

3.6 SIMULATOR PROGRAM

The simulator software is programmed by using MATLAB. It has a graphical user interface. Screenshot of the program is shown in Figure 3-8.

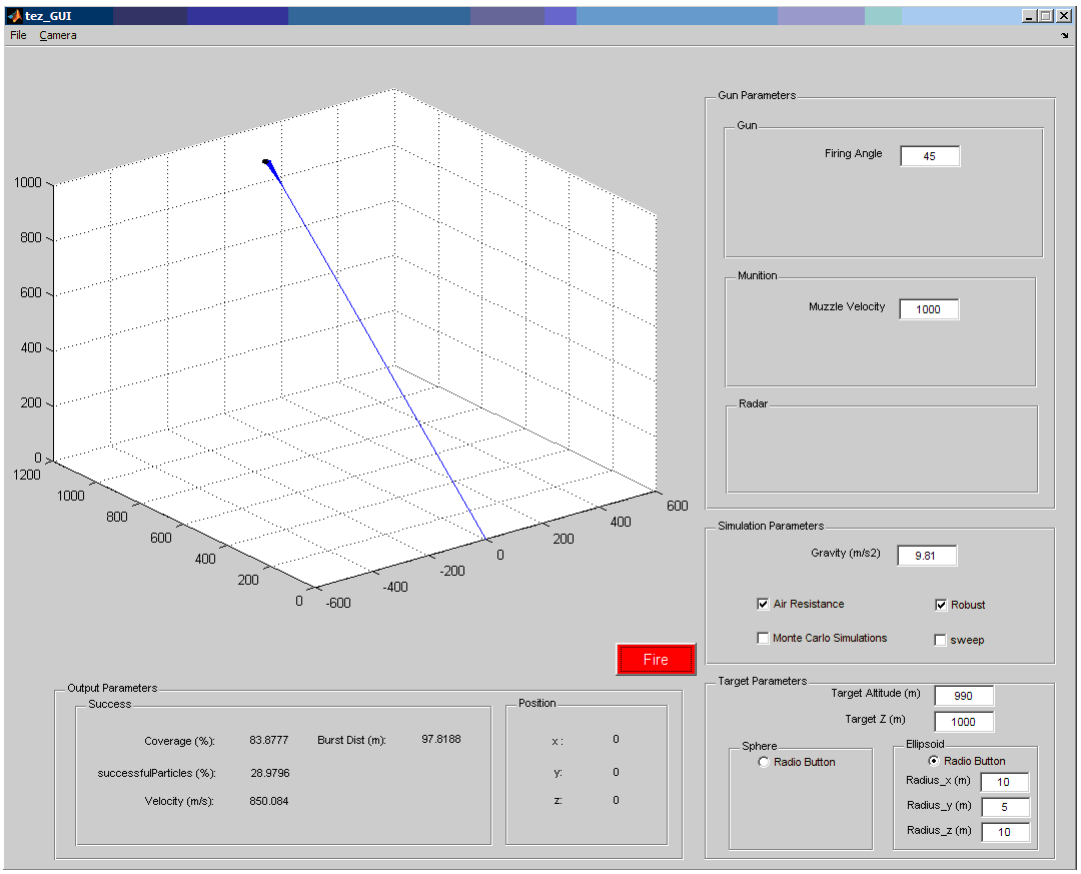

Figure 3-8: The screen shot of the simulator

The simulator program calculates the path of the munition, simulates burst, and traces the paths of the particles. The program calculates the number of particles that hit the target, it calculates the area that the munition covers on the target surface, and it gives the hit velocity of the particles to the target. Target's position ambiguity is achieved by Monte Carlo simulations. The model of the munition derived in Chapter 3.2 is directly used in the simulator. The position of the target is determined by Monte Carlo simulations as explained in the following parts. Random number generation algorithm for Monte Carlo simulation is created using Matlab function, namely randn(). This function (randn) generates random numbers whose mean is zero, variance is one. In this study, random number generation is done with the following formula: "mean + variance*randn(1)". Hence, random numbers generated by Monte Carlo simulations (errors on the target position) have Gaussian probability density function.

By using Equation(3-14) and Figure 3-4, the relation between azimuth and elevation angles can be found in order to model the cone shaped distribution of the sub-projectiles. This condition is satisfied by the Equation (3-17).

$$\frac{|AB|}{|AD|} = \cos(\phi)\cos(\varphi) \tag{3-17}$$

Since cone shaped distribution exists, $|AD|$ is constant for the same cosine multiplication angles ($\cos(\phi)\cos(\varphi)$). $|AB|$ is the burst distance, thus it is constant. According to 3-17, the relation between elevation angle and azimuth angle is derived, which indicates that multiplication of cosines of the angles is constant.

The target cross-section seen by the munition is illustrated in Figure 3-9 and is determined by Equation (3-18).

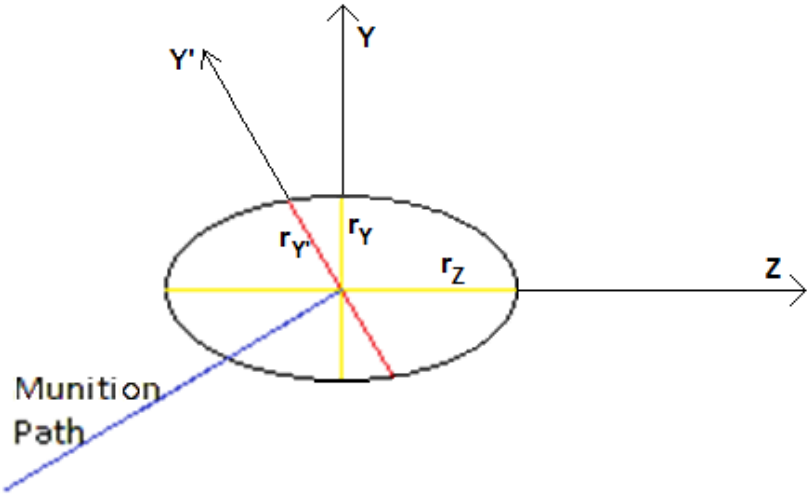

Figure 3-9: The illustration of the target cross-section seen by the munition at Y-Z axis

$$\frac{z^2}{r_Z^{\,2}} + \frac{y^2}{r_Y^{\,2}} = 1$$

$$z = -r_{Y'} \sin\theta$$
$$y = r_{Y'} \cos\theta$$

$$\frac{(-r_{Y'} \sin\theta)^2}{r_Z^{\,2}} + \frac{(r_{Y'} \cos\theta)^2}{r_Y^{\,2}} = 1$$

$$r_{Y'} = \frac{r_Z r_Y}{\sqrt{r_Z^2 \cos\theta^2 + r_Y^2 \sin\theta^2}} \tag{3-18}$$

In Equation (3-18), z and y are the coordinates of the point that red line intersects the upper half of the ellipse. r_Z is the radius of the target in the Z axis. r_Y is the radius of the target in the Y axis. $r_{Y'}$ is the radius of the cross-section seen by the munition in the Y axis with respect to the rectangular coordinate system with the origin of coordinates located at the intersection point of the munition path and the target. Coverage calculation is done by using an image processing function of MATLAB. To calculate coverage, an area is defined whose geometric sizes are

determined by using probable errors and dimensions of target as in the Equation(3-19).

$$X' = 2(r_X + \Delta r_X)$$
$$Y' = 2(r_{Y'} + \Delta r_{Y'}) \qquad (3\text{-}19)$$

X' and Y' are the magnitudes of the sides of the area. r_X is the radius of the target in the X axis and Δr_X is the magnitude of the max error in the X axis. Then two zero matrices are defined with the sizes of the area found in Equation(3-19). The random middle point which is found by Monte Carlo simulation is put on one of the matrix. This point is the center of the ellipse with radiuses rX and r_Y'. The other matrix is for saving munition's covered area. Both of the matrices represent the same area perpendicular to the path of the munition.

Then particle positions are combined by roiPoly function of the Image Processing Toolbox of the MATLAB to define the area that munition covers. Then, bitwise AND operation is performed for these matrices. Thus, covered area by the munition on target surface is found. Figure 3-10, 3-11, and 3-12 show the images in sequence to describe coverage calculation better.

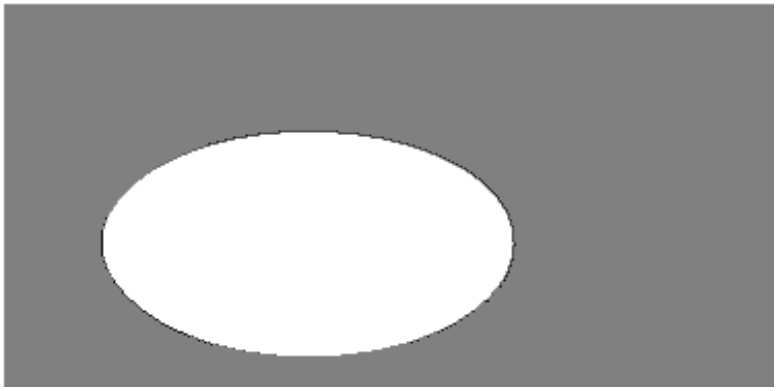

Figure 3-10: Target area which is seen on the path of the munition

In Figure 3-10, target is placed to the matrix. The elliptic area is one, grey part is zero in the matrix. This elliptic area represents the target area seen by the munition.

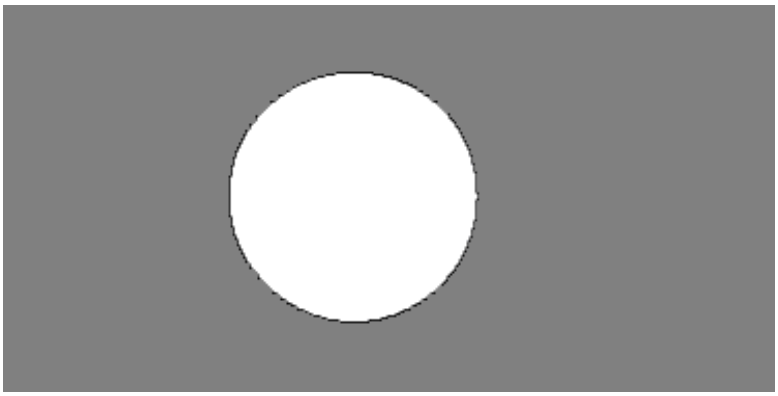

Figure 3-11: Area covered by munition

In Figure 3-11, covered area by the munition is set to one and the rest is zero.

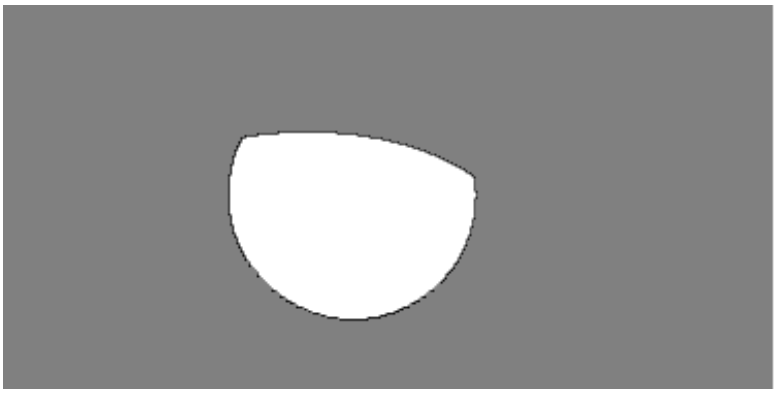

Figure 3-12: The intersection of the target and area covered by munition

In Figure 3-12, the intersection area of Figure 3-10 and Figure 3-11 is shown. This area is achieved by performing bitwise AND operation between target area and covered area of the munition as described in Figure 3-13.

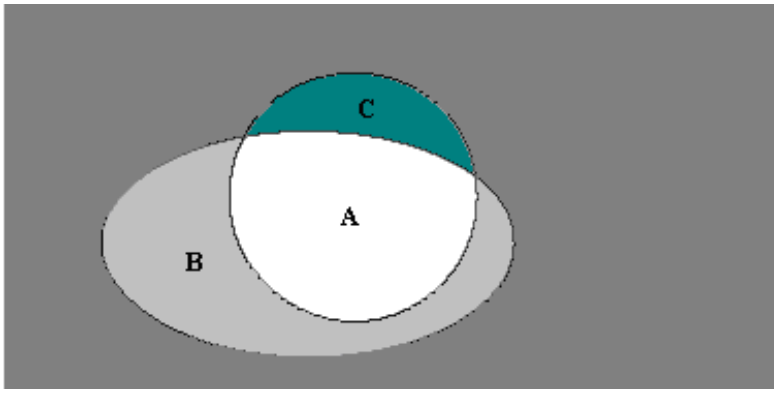

Figure 3-13: The description of the covered area

In Figure 3-13, A is the intersection of target area (Figure 3-10) and area covered by munition (Figure 3-11). B is the target area not covered by munition. No damage is done to that part of the target. C is the covered area that does not cover any target area.

The aim throughout the study can be summarized by making use of the Figure 3-13 as increasing A, decreasing C and B as much as possible.

CHAPTER 4

ANALYSIS AND SIMULATIONS

In this part, results of the simulations to find optimum burst distance are presented. Furthermore, the parameters that affect optimum burst distance are analyzed. Throughout the simulations, burst distances are swept by changing burst time. The increment between burst distances is about 1 m. Hence, the accuracy of burst distance is 1 m. However, calculated burst distances, which belong to that burst time, naturally have fractions which is not meaningful when accuracy is 1 m. To eliminate this situation, found burst distances from the simulations are rounded to integers at this chapter.

As known from Chapter 3, the coordinate system used during the simulations is Cartesian coordinate system which is given in Figure 4-1.

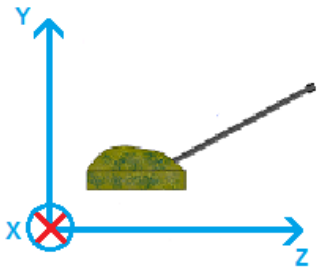

Figure 4-1: A representative figure of coordinate system

In Section 4.1, the effect of firing angle on burst distance is simulated and results are presented by a graph. In Section 4.2, target distance from the gun is changed to see the effect of that on burst distance. In Section 4.3, dimension of the target is

changed and change in the burst distance with respect to target dimension is presented. In the next section, effects of the weights of the optimization function on burst distance are analyzed separately and results are presented with graphs. In Section 4.5, effect of the ambiguity in target location on burst distance is analyzed and results are presented. In the next part, the effect of the wind on burst distance is simulated in three different ways; wind against movement, wind supports movement, and side wind. The change in the burst distance with respect to wind velocity is graphed and presented. In Section 4.7, the effect of the velocity difference after burst on optimum burst distance is analyzed. In Section 4.8, a scenario is built without ambiguities and burst distance is found. Moreover, the result of the firing method is compared to the optimum burst distance. In the last part, a scenario is simulated such that there are ambiguities in target position burst velocity. Burst distance is then calculated in the presence of such ambiguities. Furthermore, the result of the firing method is compared to the optimum burst distance.

4.1 THE EFFECT OF FIRING ANGLE

An important part of the simulations is the effect of firing angle on burst distance. Firing angle, also known as elevation angle, is the angle between gun turret and ground as shown in Figure 4-2.

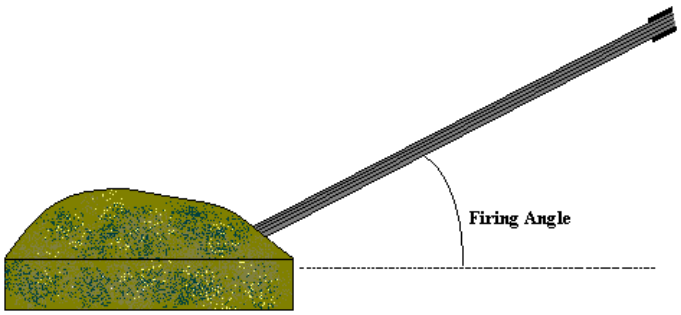

Figure 4-2: A representative figure of firing angle

Five different firing angles; 15, 30, 45, 60, and 75 degrees are simulated respectively with the following cost function defined in Chapter 3:

$$C = (\max\_hitVelocity - actual\_hitVelocity)^2 + (100 - actual\_Coverage)^2 + (181 - actual\_numberOfParticles)^2$$

The intersection point of the munition path and the target path is assumed as 1000 meters away from the gun which is represented by 'r' in Figure 4-3.

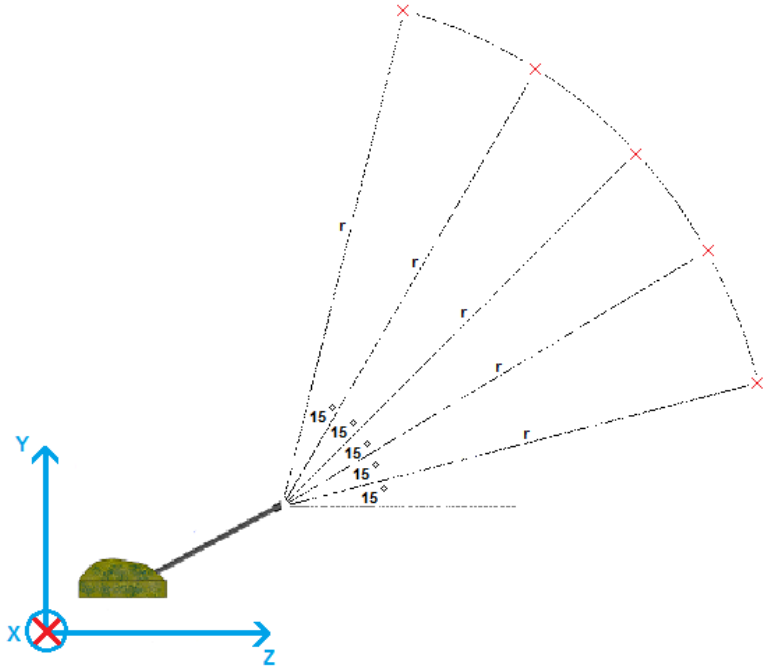

Figure 4-3: An illustration of firing angle simulation

Dimensions of the target are taken as follows: X radius is 10 m, Y radius is 5 m, and Z radius is 10 m. The results of this simulation are presented in Figure 4-4 which shows the change in burst distance with respect to firing angle.

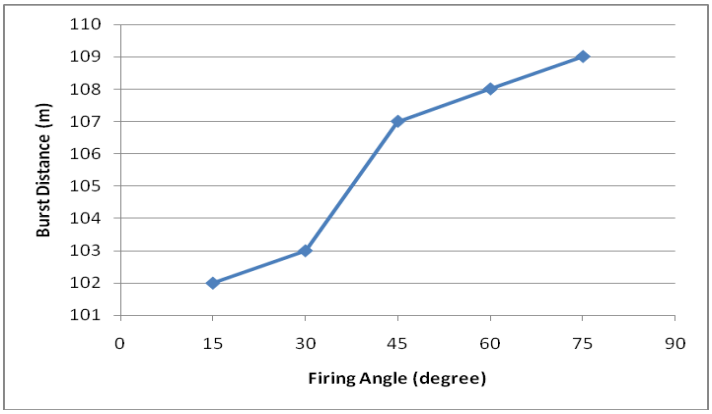

Figure 4-4: The effect of firing angle on optimum burst distance

As shown in Figure 4-3, firing angles are changed from 15 degrees to 75 degrees. At 15 degrees burst distance is 102 m and at 75 degrees burst distance is 109 m. From these simulations, it is seen that burst distance increases with firing angle. This is an expected result, since cross-sectional area of the target increases with angle which is clear by Equation (3-18) and burst distance increases with cross-sectional area as given in Section 4.3.

Table 4-1: Deviation weights of the objective parameters in total deviation

Firing angle (degree)	Optimum burst distance (m)	Deviation square in velocity	Deviation square in coverage	Deviation square in # of particles	Total cost value
15	102	6.068587783	95.40991684	417.8749122	519.3534
30	103	4.786675932	11.44062976	147.7366381	163.9639
45	107	3.58671553	2.66799556	30.52409878	36.77881
60	108	2.866533328	2.20314649	2.74716889	7.816849
75	109	2.400559934	2.48314564	0.305240988	5.188947

To observe the contribution of each error terms to the total cost value, a table (Table 4-1 given on the previous page) is constructed. The table shows the firing angle, the corresponding optimum burst distances, the individual error squares, and finally the total optimum cost value. It can be easily observed that the total cost value, and the cost due to number of particles hitting the target decreases dramatically as the firing angle increases. This is an expected result, because as firing angle increases the cross sectional area of the target facing the particles increases.

4.2 THE EFFECT OF RANGE

The effect of the range of the target on the burst distance is an important part of the simulations. The dimensions of the target used during the simulations are the same as in Section 4.1. Range in these simulations stands for the distance between the gun and the intersection point of the munition path and the target path. Five different ranges are simulated in this part to see the change in the burst distance. These ranges correspond to very short range air defense in real life, as in the case of a demonstration of 35 mm airburst munition handled by Army Research Laboratory [2]. These simulated ranges are: 500 m, 1000 m, 1500 m, 2000 m, and 2500 m at 45 degrees of firing angle. Figure 4-5 shows the change in burst distance with respect to range.

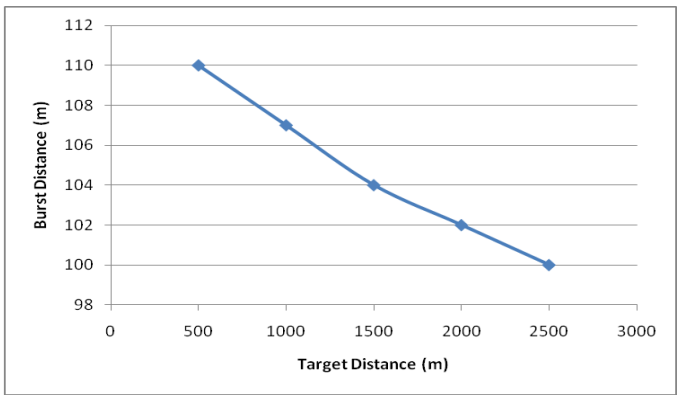

Figure 4-5: The effect of range on optimum burst distance

As shown in Figure 4-5, ranges are changed from 500 m to 2500 m. When range is 500 m burst distance is 110 m and when range is 2500 m burst distance is 100 m. Thus, it is inferred from these simulations that burst distance decreases with ranges which is expected. Angle of the munition with respect to ground decreases on the trajectory with range. Hence, opposite of Section 4.1, burst distance decreases with decreasing angle.

4.3 THE EFFECT OF THE TARGET DIMENSIONS

The effect of the target dimensions on burst distance is another important part of the simulations. Since target is modeled as an ellipsoid, dimensions are the radii in X, Y, and Z axes. Simulations at this part are handled for five different target dimensions. The radii are stated in the (x, y, z) format; (5, 3, 5), (10, 5, 10), (15, 7, 15), (15, 15, 15), and (20, 10, 20). Firing angle is 45 degrees during the simulations. Moreover, hit point, intersection of the munition path and the target path, is chosen as 1000m from the gun. Figure 4-6 shows the change in burst distance with respect to target volume.

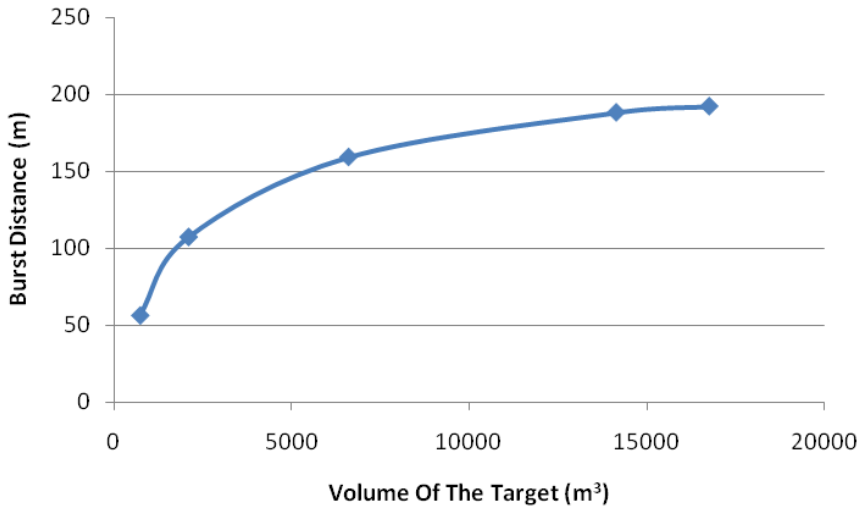

Figure 4-6: The effect of target dimensions on optimum burst distance

If target area increased with the same burst distance, coverage would decrease. To increase coverage objective, burst distance should be increased. According to Figure 4-6, burst distance increases with target dimensions which is an expected result. If target dimension increases, burst distance will increase.

4.4 THE EFFECTS OF THE WEIGHTS IN THE COST FUNCTION

In this part, the effects of the weights of the cost function on optimum burst distance are analyzed. Initially, the weights of the objective parameters are equal to 1. Effect of an objective parameter is simulated, while weights of the other objective parameters are kept constant. Firing angle is 45 degrees during the simulations. Hit point, intersection point of the munition path and the target path, is taken as 1000 m from the gun. Dimensions of the target are the same as in Section 4.1. Figure 4-7 is the graph of equal weight cost function with respect to burst distance. Optimum burst distance is 107 m.

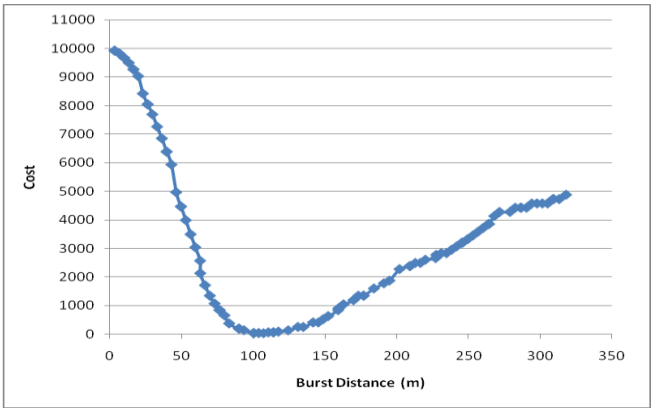

Figure 4-7: The graph of equal weight cost function with respect to burst distance

Targets with stronger skin are hard to damage. Particles should hit with higher velocity to these kinds of targets. Hence, this makes the importance of the hit

velocity higher. Figure 4-8 shows the change in burst distance with increasing velocity weight in the cost function.

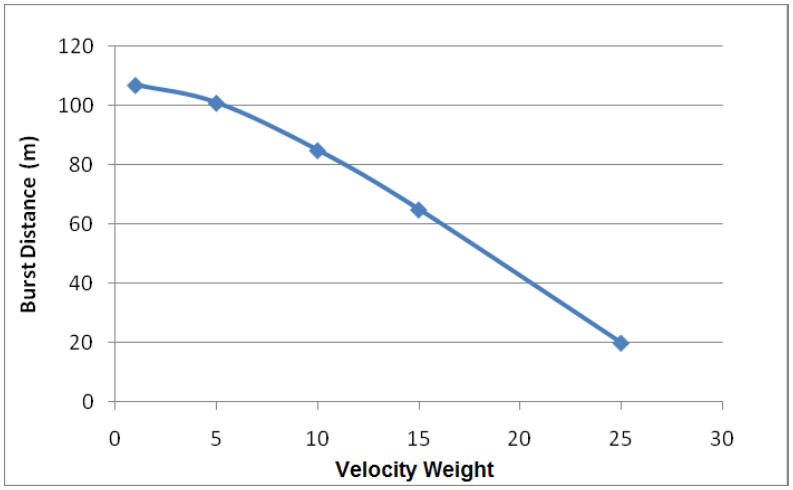

Figure 4-8: The change in burst distance with increasing velocity constant

If burst distance increases, hit velocity will decrease. Thus, if bigger hit velocity is demanded, burst distance will decrease. Parallel to the expectations, burst distance is decreasing with increasing hit velocity weight. Thus, results given in Figure 4-8 are not surprising.

When the weight of coverage is increased, the change in burst distance is given by Figure 4-9.

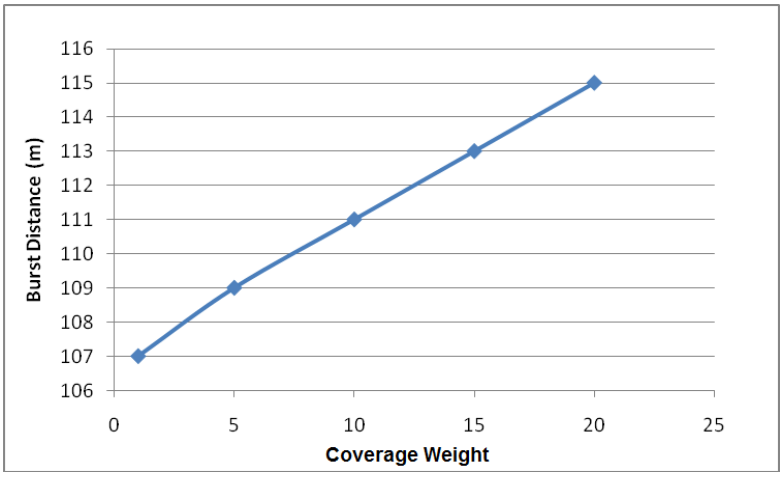

Figure 4-9: The change in burst distance with increasing coverage constant

If burst distance increases, coverage will increase. Thus, if bigger coverage is demanded, burst distance will increase up to a burst distance when coverage is 100%. Hence, the results of Figure 4-9 are as expected.

When the weight of particles that hit the target is increased, the change in burst distance is given by Figure 4-10.

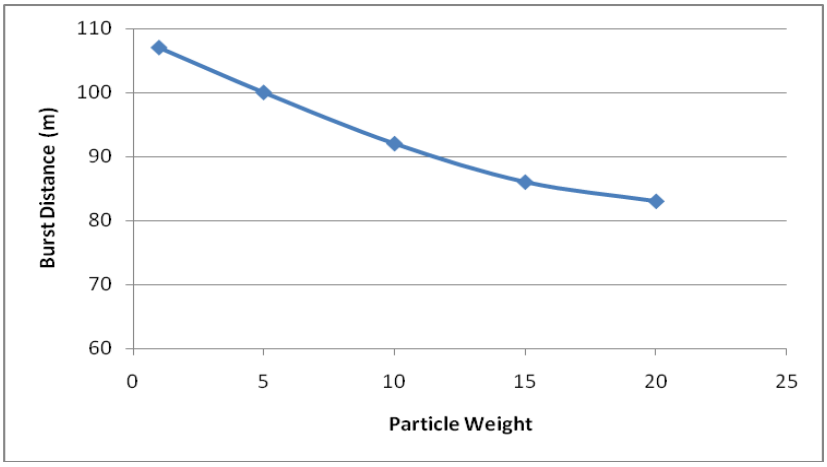

Figure 4-10: The change in burst distance with increasing particle constant

If burst distance increases, number of particles that hit the target will decrease. Therefore, to increase the number of particles that hit the target, burst distance will decrease until all particles hit the target. Thus, Figure 4-10 gives expected results.

4.5 THE EFFECTS OF AMBIGUITY IN TARGET LOCATION

Due to the radar errors, target position estimation errors, mechanical errors etc. some amount of ambiguity in the target position occurs. At this part, the effect of the ambiguity in the target location on optimum burst distance is observed. The ambiguity in the target location is modeled as a Gaussian distribution. However, the ambiguity in the target location differs from system to system. These simulations show the change in optimum burst distance with respect to ambiguity.

During simulations, firing angle is set to 45 degrees. Hit point, which is the intersection point of the munition path and the target path, is selected as 1000 m away from the gun. The dimensions of the target are the same as in Section 4.1. Five different variances are chosen for target location ambiguity, which is assumed to be Gaussian distributed. These variances in X and Y coordinates are stated as (X, Y) format; namely (5, 2.5), (10, 5), (15, 7.5), (20, 10), and (25, 12.5). Figure 4-11 shows the change in the burst distance with respect to the ambiguity in the target location. 1, 2, 3, 4, and 5 refers to the variances mentioned above in the same order.

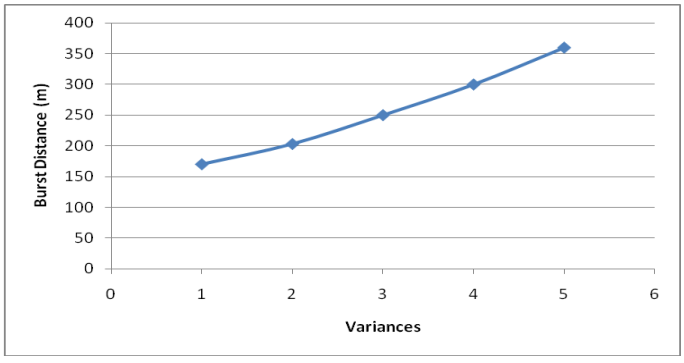

Figure 4-11: The change in burst distance with increasing variance

If ambiguity in target location increases, hit probability will decrease. To increase hit probability, burst distance should be increased. That makes Figure 4-11 reasonable.

4.6 THE EFFECT OF WIND

In this part, the effect of wind on optimum burst distance is observed. Depending on the wind velocity and direction, munition path may change a lot, even target may be missed. However, in these simulations such exceptional cases are not handled. Wind velocity is changed from zero to 30 m/s. Simulations are done for 45 degrees firing angle. Hit point, intersection point of the munition path and the target path, is 1000 m away from the gun. The dimensions of the target are the same as in Section 4.1. Figure 4-12 shows the change in burst distance with respect to wind against movement on Z axis.

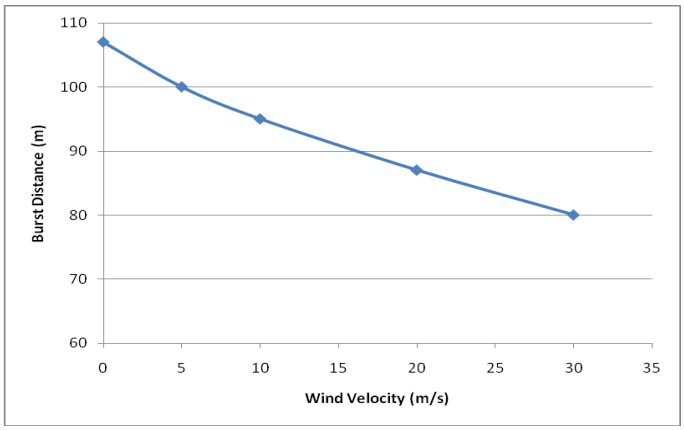

Figure 4-12: The change in burst distance with increasing wind velocity against the movement on Z axis

According to the results presented in Figure 4-12, optimum burst distance decreases with increasing wind velocity against the movement on Z axis.

Figure 4-13 shows the change in the burst distance with respect to wind in the movement direction on Z axis.

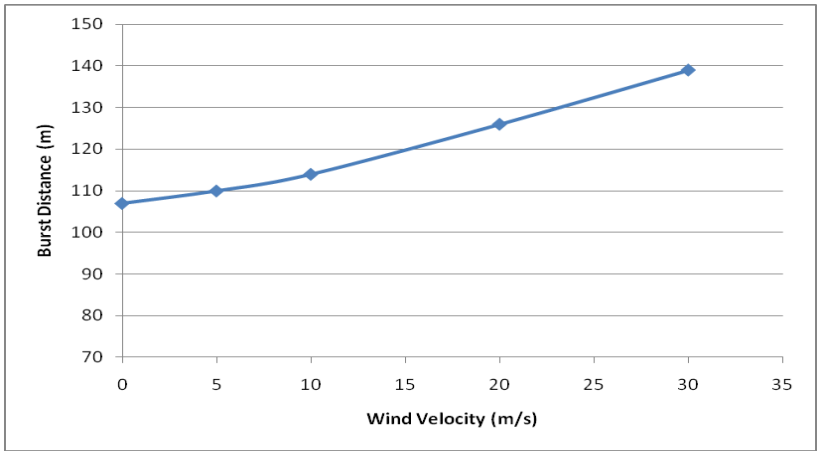

Figure 4-13: The change in burst distance with increasing wind velocity in the same direction with the movement on Z axis

According to the results presented in Figure 4-13, optimum burst distance increases with increasing wind velocity in the same direction with the movement on Z axis.

Figure 4-14 shows the change in the burst distance with respect to the wind on the X axis.

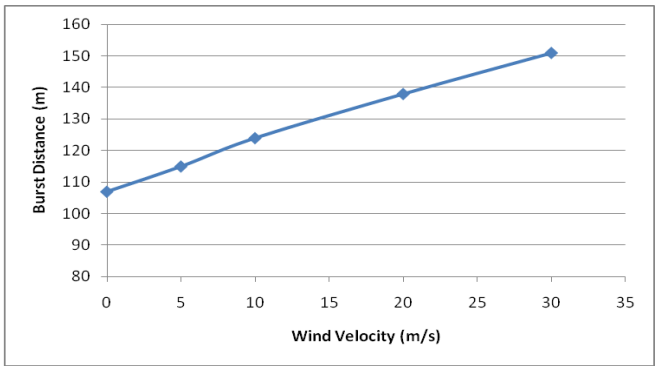

Figure 4-14: The change in burst distance with increasing wind velocity on X axis

According to the results presented in Figure 4-14, optimum burst distance increases with increasing wind velocity along X axis.

4.7 THE EFFECT OF VELOCITY AMBIGUITY AFTER BURST

In this part, the effect of velocity ambiguity after burst on optimum burst distance is observed. The dimensions of the target used in these simulations are the same as in Section 4.1. During the simulations, firing angle is 45 degrees. Hit point, intersection point of the munition path and the target, is 1000 m away from the gun. As it is known from Section 2.5, muzzle velocity ambiguity is a well known subject. It is studied a lot. Any variance in muzzle velocity changes the burst position which means optimum burst distance is not conserved. Thus, effectiveness decreases. However, velocity ambiguity after burst is not mentioned at these studies. Figure 4-15 shows the change in the burst distance with respect to different velocity increments due to burst.

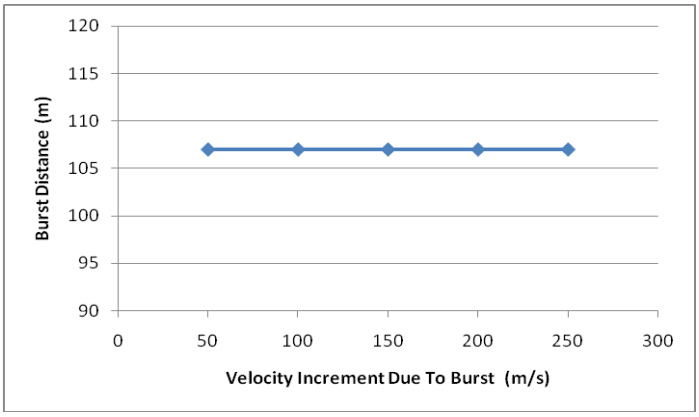

Figure 4-15: Change in the burst distance with respect to different velocity increments due to burst

Particles gain some velocity due to burst. In Figure 4-15, these gained velocities are changed from 50 m/s to 250 m/s to see the change in the optimum burst distance. As it can be seen from Figure 4-15, optimum burst distance is not influenced from

the variation of the velocity increment after burst. However, effects of the particles are influenced from variation as seen in Figure 4-16.

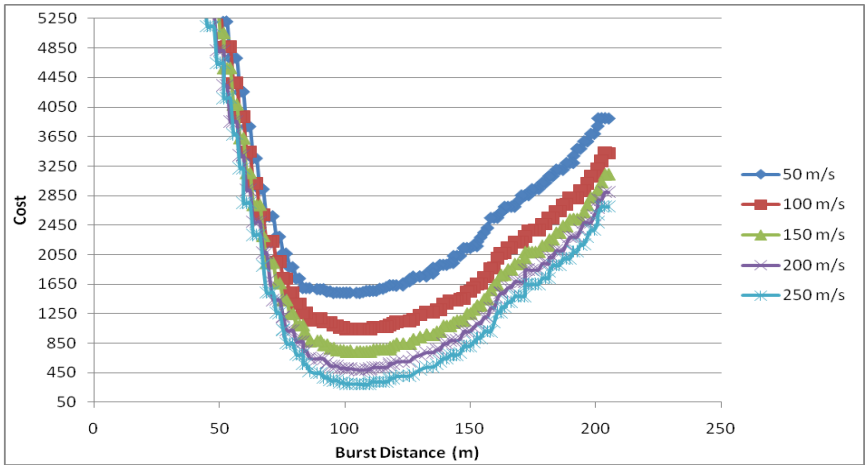

Figure 4-16: Change in the cost value with respect to different velocity increments due to burst

Higher the velocity increment, higher hit velocity. Thus, particles have more kinetic energy which means they are more effective.

4.8 SIMULATION WITHOUT AMBIGUITY

In this part, we assume that the target position is known perfectly and burst velocity increase is 150 m/s. Simulation parameters are; 45 degrees firing angle, intersection point of the munition path and the target path is 1000 m away from the gun. Dimensions of the target are the same as the other simulations. Figure 4-16 shows the burst distance cost value graph of the simulation result.

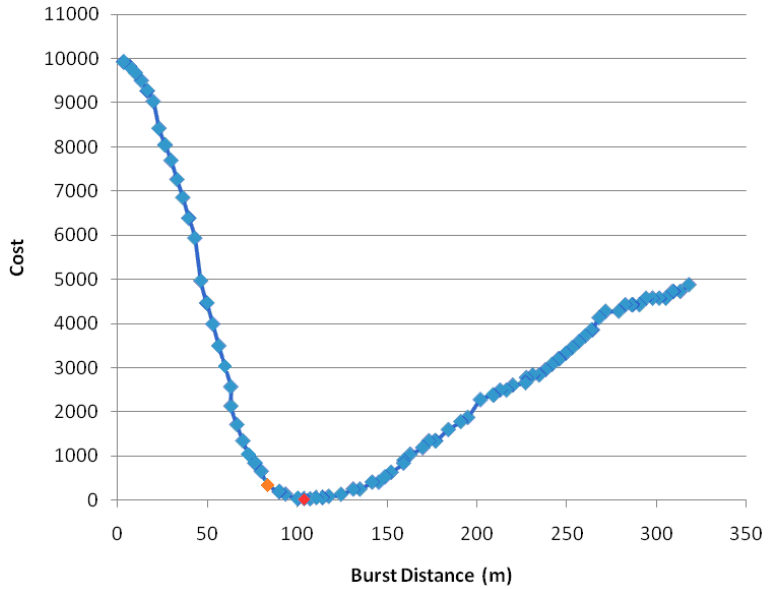

Figure 4-16: Burst distance cost value graph. Optimum burst distance and the solution of the proposed method are also indicated

Red point shows the optimum burst distance at Figure 4-16 and orange point shows the solution of the "firing method" which is the method applied when there is no ambiguity in the target position (method presented in Section 3-4). Optimum burst distance with respect to equal weight cost function is 107 m. The result of the firing method for this case is 83 m. The success of the firing method is calculated by assigning 0% success to the worst point (cost value 10000) and 100% success to the optimum burst point. Hence, the success of the firing method according to the mentioned calculation is 96.5%.

Table 4-2: Objective parameters of the optimum solution and the solutions of the firing methods.

	HIT VELOCITY (m/s)	NUMBER OF PARTICLES THAT HIT THE TARGET	COVERAGE (%)
Red Point (Optimum Solution)	642.3664	168	100
Orange Point (Solution of the firing method)	645.2374	181	80.8659

4.9 SIMULATION WITH COMPLETE MODEL

In this part, simulation is done including target position ambiguity and velocity ambiguity. Simulation parameters are; 45 degrees firing angle, intersection point of the munition path and the target is 1000 m away from the gun. Random numbers generated for Monte Carlo simulations have zero mean, 10 m variance for X axis, and 5 m variance for Y axis for target position; zero mean, 10 m/s variance for velocity. 700 Monte Carlo simulations are conducted the average of which is shown in Figure 4-17. In the figure, the variances observed in simulations are also indicated (vertical orange lines).

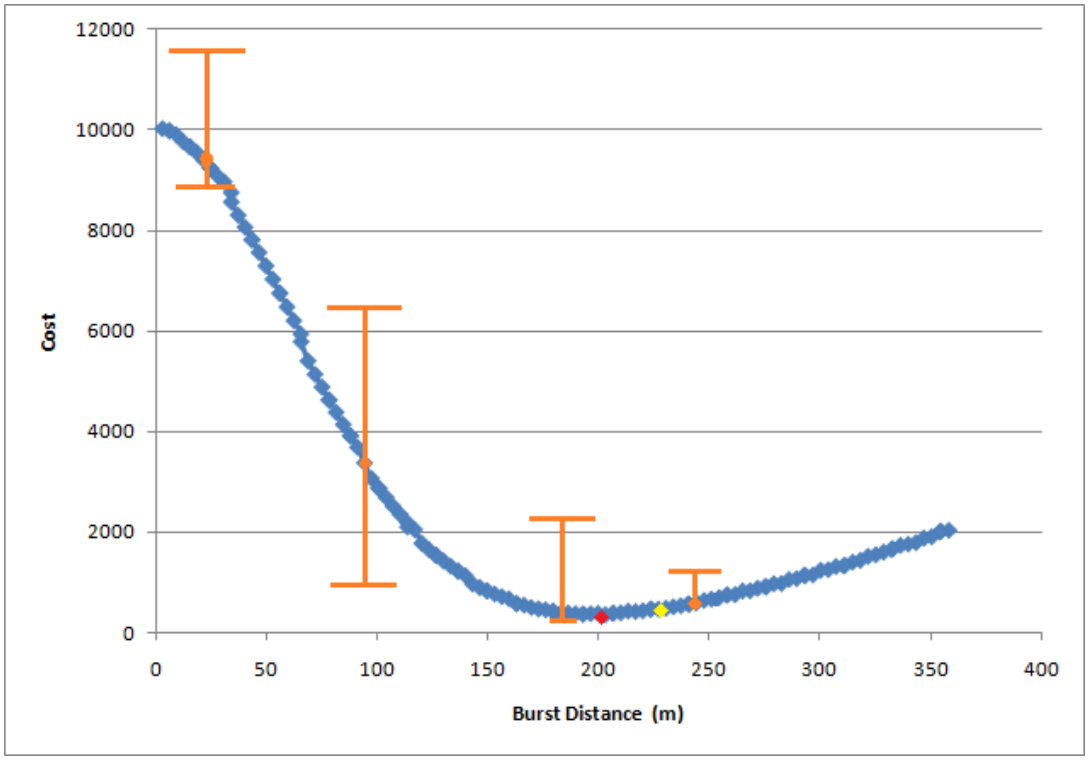

Figure 4-17: Burst distance cost value graph. Optimum burst distance and firing method solution are also indicated

Red point shows the optimum burst distance in Figure 4-17 and yellow point shows the solution of the "firing method". Optimum burst distance with respect to equal weight cost function is 203 m. The result of the firing method for this case is 235 m. The success of the "firing method" is 98.3%. As seen from the figure, variance from the average is high for burst distances smaller than the optimum burst distance. This can be explained by the fact that, for burst distances bigger than the optimum burst distance, the coverage of the munition is enough to tolerate the errors of target position.

Table 4-3: Objective parameters of the optimum solution and the "firing method" solution.

	HIT VELOCITY (m/s)	NUMBER OF PARTICLES THAT HIT THE TARGET	COVERAGE (%)
Red Point (Optimum Solution)	635.75	146.27	88.54
Yellow Point (Solution of the firing method, when target position is not known precisely)	632.13	134.41	93.44

CHAPTER 5

CONCLUSION AND FUTURE WORK

5.1 CONCLUSION

Airburst munitions are effective for very short range air defense. In the literature, there are some studies to increase the effectiveness of airburst munitions. However, all of these studies assume an optimum burst distance exists and try to maintain these optimum burst distances. In this thesis, calculation of optimum burst distance is analyzed as an optimization problem and a way to calculate optimum burst distance is presented. The parameters that effect optimum burst distance are analyzed by simulations. Furthermore, a firing method is proposed.

The parameters that may affect optimum burst distance are firing angle, range of the target, dimensions of the target, presence of wind, importance of the objectives, ambiguity in the target position, and variation of the particle velocities after burst. According to the simulation results, it is seen that the burst distance becomes bigger with increasing target dimensions. The relation between the firing angle and the burst distance is proportional. Burst distance increases with firing angle. Therefore, if target range increases, burst distance decreases. If ambiguity of the target position increases, burst distance will increase. Depending on the target attributes, importance of the objectives change. If hit velocity is more important, burst distance will decrease. Similarly, burst distance decreases with increasing importance of the number of particles that hit the target. Conversely, if coverage is more important, burst distance will increase. Furthermore, the affect of wind on optimal burst distance is simulated. Side winds and winds that assist the movement of the munition increase optimal burst distance. On the contrary, winds that oppose

movement of the munition decrease optimal burst distance with increasing wind velocity. Moreover, velocity variation after burst is also simulated to see how it affects burst distance. However, it has no influence on burst distance. The variation on the velocity after burst changes the effects of the particles.

In addition to simulation results mentioned, comparison of the firing methods with optimal solution is presented. The success of the proposed firing method without any ambiguity in the system and target location has been calculated as 96.6%. If the errors are included, such as target position ambiguity and velocity ambiguity due to burst, the success of the proposed firing method has been calculated as 98.3%.

At the beginning of the study, the motivation was to discover a method to find optimum burst distance for increasing air defense capability. Now, at the end of the study, the followings are achieved; knowledge about the factors that affect optimum burst distance, a way to calculate optimum burst distance with a target dependent cost function, and a firing method which can be used without calculating burst distance.

5.2 FUTURE WORK

A more realistic target may be used during the simulations. Some parts of the target may have different importance, like in the real world. Hence, simulations may be repeated and some tuning to burst distance may be done.

Moreover, rotational munition may be used during the simulations whose angle of attack, shown in Figure 3-1, is non zero. Simulations may be repeated and some tuning to burst distance may be done. Furthermore, a changing wind with respect to altitude may be added to see the difference.

Another possible extension to this study is simulating effects of firing patterns. Firing patterns may have significant effect in real world situations. Depending on the firing pattern, optimum burst distance may change.

REFERENCES

[1] US Army Armament Research, Development and Engineering Center, MIL HDBK 799, “Department of Defence Handbook”, Fire Control Systems, 5 April 1996.

[2] Timoty G. Farrant, “Results of 35mm Airburst Demonstration”, Army Research Laboratory, January 2000.

[3] Major Mark W. Richter, ”The Operational Effectiveness of Medium Caliber Airburst Munitions”, US Marine Corps, 2002.

[4] Cyrus F. Wood, “Review of Design Optimization Techniques”, IEEE Transactions on Systems Science and Cybernetics, Page(s): 14-20, November 1965.

[5] Jorge Nocedal and Stephen J. Wright, "Numerical Optimization", Springer, 2006.

[6] Andre Boss, US 6427598 , “Method and Device for Correcting the Predetermined Disaggregation Time of a Spin-Stabilized Programmable Projectile”, Oerlikon Contraves, August 2002.

[7] Peter Toth, US 5322016, “Method for Increasing the Probability of Success of Air Defense by Means of a Remotely Fragmentable Projectile”, Oerlikon Contraves, June 1994.

[8] Andre Boss, US 5814756 , “Method and Device for Determining the Disaggregation Time of a Programmable Projectile” Oerlikon Contraves, September 1998.

[9] C. Wachsberger, M. Lucas,A. Krstic,” Limitations of Guns as a Defence against Manoeuvring Air Weapons”,Australian Government Department of Defence, Systems Sciences Laboratory, June 2004.

[10] A.Buckley, “40mm x 53 Air Burst Munition for Automatic Grenade Launchers”, 47th Annual Fuze Conference “Enhancing Weapon Performance“, New Orleans, LA – April 8-10, 2003.

[11] E.Elmer,” 30mm Air Bursting Munitions for the MK44 Cannon”, 2008 NDIA Gun and Missile Systems Conference & Gun Exposition, 21 - 24 April 2008.

[12] A. Boss, US 64221119 , “Method and Device for Transferring Information to Programmable Projectile”, Oerlikon Contraves, July 2002.

[13] Andre Boss, US 5834675 , “Method for Determining the Disaggregation Time of a Programmable Projectile”, Oerlikon Contraves, November 1998.

[14] D. Andersen, D. Wright, “Advanced Crew Served Weapon (ACSW)–XM307; Ammunition Crew Safety & Precision Air-Burst”, NDIA Fuze Conference, Seattle, Washington,April 2005.

[15] ATK, “Air Bursting Munitions”, The 36th Annual Gun & Ammunition Symposium, San Diego, CA, April 9 - 12, 2001.

[16] J.J.M. Paulissen, E. van Meerten, Th.L.A. Verhagen, “Effectiveness of Air Burst Munitions”, 44th NDIA GMS, 9 April 2009 .

[17] B. Harris, M. Walker, “Joint Gun Effectiveness Model”, National Defense Industrial Association Gun and Missile Systems Conference & Exhibition, Sacramento Convention Center, Sacramento, CA, March 27-30, 2006.

[18] K. P. Werrell, “A Short Operational History of Ground-Based Air Defense”, Air University Press, Maxwell Air Force Base, Alabama, Second Edition, August 2005.

[19] A. Boss, TR199600952A1 , “Method for Determining the Disaggregation Time of a Programmable Projectile”, Oerlikon Contraves, November 1997.

[20] Encyclopedia Britannica, http://www.britannica.com/EBchecked/topic/222764/fuse, last visited on 20th December 2009.

[21] G.Ettel, US4672316 , “Method for Calibration a Muzzle Velocity Measuring Device”, Oerlikon-Bührle, June 1987.

[22] Hogg, OFG, "Artillery: its origin, heyday and decline", London: C. Hurst & Company,1970.

[23] Nasa, http://www.grc.nasa.gov/WWW/K-12/airplane/sized.html, last visited 24th on December 2009.

[24] Air Resistance: Distinguishing Between Laminar and Turbulent Flow, http://nautilus.fis.uc.pt/personal/pvalberto/aulas/cef_mestrado/Air.Resistance.pdf, last visited 22th on February 2010.

[25] Raymond A. S., John W. J., "Physics for Scientists and Engineers", Brooks/Cole, 2004.

[26] McCoy Robert L., Modern exterior ballistics; the launch and flight dynamics of symmetric projectiles, USA : Schiffer Publishing Ltd, 1999.

[27] J. Clayton Kerce, Divid F. Hardiman, and George C. Brown, Nonlinear Estimation Techniques for Impact Point Prediction of Ballistic Targets.

[28] Lancaster University, Methods and Benefits of Simplification in Simulation, Roger J. Brooks, Andrew M. Tobias.

[29] New York University, http://www.cns.nyu.edu/~eero/NOTES/leastSquares.pdf, last visited on 27th October 2010.

[30] Efunda, http://www.efunda.com/math/leastsquares/leastsquares.cfm, last visited on 27th October 2010.

[31] John C. Butcher, "Numerical methods for ordinary differential equations" , Wiley, 2003.